

# Violacein-Induced Chaperone System Collapse Underlies Multistage Antiplasmodial Activity

Tatyana Almeida Tavella, Noeli Soares Melo da Silva, Natalie Spillman, Ana Carolina Andrade Vitor Kayano, Gustavo Capatti Cassiano, Adrielle Ayumi Vasconcelos, Antônio Pedro Camargo, Djane Clarys Baia da Silva, Diana Fontinha, Luis Carlos Salazar Alvarez, Letícia Tiburcio Ferreira, Kaira Cristina Peralis Tomaz, Bruno Junior Neves, Ludimila Dias Almeida, Daniel Youssef Bargieri, Marcus Vinicius Guimarães de Lacerda, Pedro Vitor Lemos Cravo, Per Sunnerhagen, Miguel Prudêncio, Carolina Horta Andrade, Stefanie Costa Pinto Lopes, Marcelo Falsarella Carazzolle, Leann Tilley, Elizabeth Bilsland, Júlio César Borges, and Fabio Trindade Maranhão Costa\*

Cite This: *ACS Infect. Dis.* 2021, 7, 759–776

Read Online

ACCESS |

Metrics & More

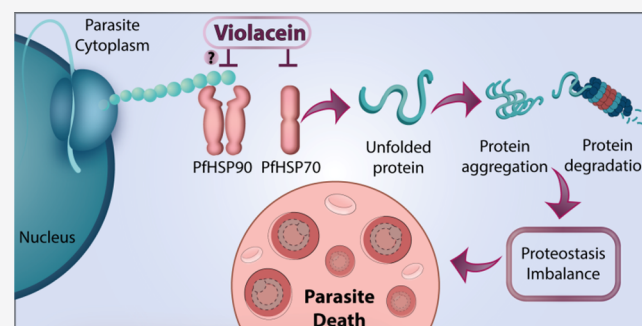
Article Recommendations

Supporting Information

**ABSTRACT:** Antimalarial drugs with novel modes of action and wide therapeutic potential are needed to pave the way for malaria eradication. Violacein is a natural compound known for its biological activity against cancer cells and several pathogens, including the malaria parasite, *Plasmodium falciparum* (Pf). Herein, using chemical genomic profiling (CGP), we found that violacein affects protein homeostasis. Mechanistically, violacein binds Pf chaperones, PfHsp90 and PfHsp70-1, compromising the latter's ATPase and chaperone activities. Additionally, violacein-treated parasites exhibited increased protein unfolding and proteasomal degradation. The uncoupling of the parasite stress response reflects the multistage growth inhibitory effect promoted by violacein.

Despite evidence of proteotoxic stress, violacein did not inhibit global protein synthesis via UPR activation—a process that is highly dependent on chaperones, in agreement with the notion of a violacein-induced proteostasis collapse. Our data highlight the importance of a functioning chaperone–proteasome system for parasite development and differentiation. Thus, a violacein-like small molecule might provide a good scaffold for development of a novel probe for examining the molecular chaperone network and/or antiplasmodial drug design.

**KEYWORDS:** malaria, chaperone inhibitor, chemogenomics, violacein, proteostasis



Malaria is one of the most prevalent human parasitic diseases, responsible for more than 400 000 deaths in 2018.<sup>1</sup> This disease is caused by infection with protozoans of the genus *Plasmodium*, which undergo striking metabolic and structural remodeling to support hepatic and blood infection cycles in the mammalian host. Mammalian infection starts with the injection of sporozoites during a blood meal of an infected female anopheline mosquito. Sporozoites reach the liver, where they infect hepatocytes and undergo schizogony, generating thousands of merozoites that are then released into the bloodstream. Within the vasculature, merozoites infect red blood cells (RBCs), remodeling host cells during the maturation of the parasite from early stages (rings) to mature stages (trophozoites and schizonts). During the final stage of schizont maturation, dozens of daughter merozoites burst from the RBCs and invade new ones. A small percentage of the asexual parasites differentiate into sexual gametocytes,

which are taken up by a feeding mosquito, thus continuing the parasite's life cycle.<sup>2</sup> The activity of most antimalarials is restricted to asexual blood stages.<sup>3</sup> Very few drugs are active against the obligatory and clinically silent liver stage of infection or against gametocytes, the only parasitic stage capable of transmitting malaria to the invertebrate host.<sup>4</sup> As such, in 2007, the Bill and Melinda Gates Foundation prioritized the discovery of drugs for malaria prophylaxis and transmission blocking, to underpin disease eradication.<sup>5</sup>

Received: June 27, 2020

Published: March 10, 2021



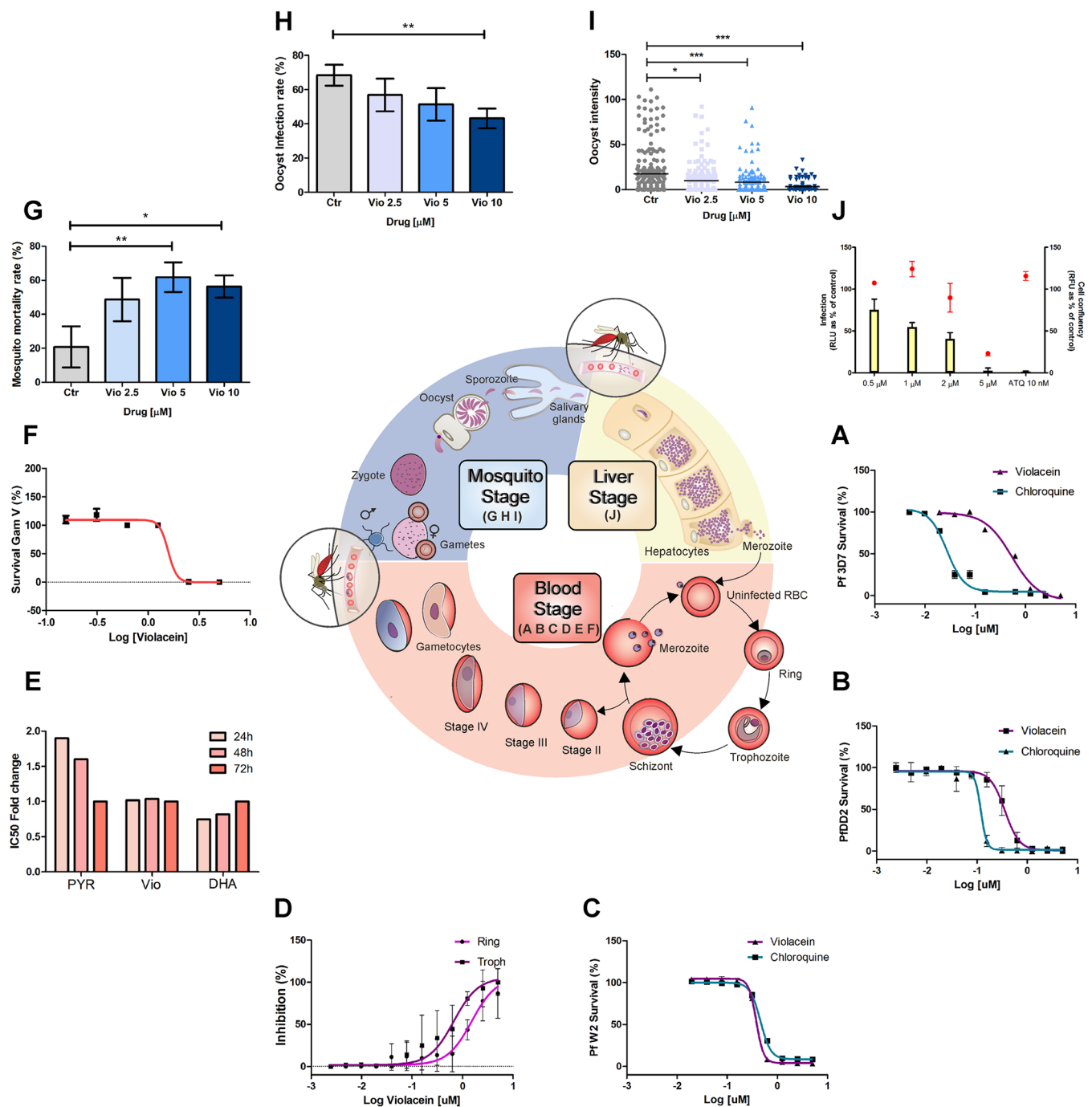


**Figure 1.** Violacein multistage antimalarial activity. (A–C) Violacein *in vitro* activity against asexual stage *P. falciparum* 3D7 strain (A) and chloroquine-resistant strains: Dd2 (B) and W2 (C). Graphs were calculated according with SYBRGreen measurements, and error bars represent SEM ( $n = 3$ ). (D) Violacein stage specificity within asexual parasites. Error bars represents SD ( $n = 3$ ). (E) Violacein speed of action. Asynchronous 3D7 parasites were treated with violacein for different times (24 and 48 h) to determine the EC<sub>50</sub> fold changes in relation to the EC<sub>50</sub> determined at 72 h. Pyrimethamine (PYR) and dihydroartemisinin (DHA) were used as controls for slow and fast killing compounds, respectively. The data represents one independent experiment (with internal replicates  $n = 3$ ). (F) Violacein activity against stage V gametocytes; violacein EC<sub>50</sub> = 2.5 and 1.25  $\mu\text{M}$ . The data represent the means  $\pm$  SD ( $n = 3$ ). (G) *Anopheles aquasalis* mosquitoes were fed with blood samples collected from patients infected with *P. vivax* supplemented with different concentrations of violacein. Compound insecticide activity was evaluated as the relation between dead and fed mosquitoes. The data represent the means  $\pm$  SEM ( $n = 6$ ). (H) Oocyst infection rates were determined as a relation between infected and fed mosquitoes. The data represent the means  $\pm$  SEM ( $n = 6$ ). (I) Oocyst intensity in violacein treated groups. Dots represent oocyst counts present in the midgut of each dissected mosquito; solid lines represent mean values of oocyst counts found in mosquito groups fed with blood submitted to different violacein treatments. The data represent the means  $\pm$  SEM ( $n = 6$ ). (J) Inhibition of *P. berghei* hepatic infection in vitro by violacein. Atovaquone (ATO) was used as a positive control. The data represent the means  $\pm$  SD of triplicates ( $n = 1$ ). The bars represent parasite load, assessed by the relative luminescence 48 h after infection of Huh7 cells with luciferase-expressing *P. berghei* sporozoites, whereas the dots represent cell confluency.

Cell viability relies on protein quality control processes that ensure that essential proteins are maintained in correctly folded, functional tertiary structures. Ensuring proteostasis in a cellular environment, where protein concentrations can reach >300 mg/mL,<sup>6</sup> is a challenging task that, if unbalanced, can lead to protein aggregation and denaturation. Cells use molecular chaperones, powered by ATP hydrolysis, to ensure efficient protein folding and repair.<sup>7–9</sup> In addition to regular cellular stresses, *Plasmodium* parasites have to deal with the toxic reactive oxygen species and free heme that is released during hemoglobin digestion.<sup>10</sup> These parasites must also accommodate a ~10 °C temperature change during transmission from the *Anopheles* mosquito to the mammalian host, as well as the ensuing febrile episodes in the host. Unsurprisingly, genes encoding proteins of the chaperone system comprise ~2% of the parasite's genetic repertoire.<sup>11–13</sup> Nonetheless, the parasite has only a rudimentary unfolded protein response.<sup>14,15</sup> Given that chaperones are essential at multiple stages of the parasite's life cycle,<sup>20–23</sup> insufficiencies in these folding machineries could be the *Plasmodium* Achilles' heel.<sup>18</sup>

Over the past 200 years, natural compounds have been exploited for malaria chemotherapy and control.<sup>20–23</sup> Violacein is a natural compound that is produced by the secondary metabolism of Gram-negative bacteria (e.g., *Chromobacterium violaceum*) and that exhibits broad biological activity against cancer cells, as well as against viral, parasitic, and bacterial microorganisms.<sup>24–26</sup> Violacein was shown to reduce malaria parasitemia *in vivo* and to provide ~80% protection in mice infected with a lethal strain of *P. chabaudi chabaudi*.<sup>27</sup> Despite its high activity against several pathogens, violacein has a relatively low selectivity index (varying between 3- and 20-fold), when comparing EC<sub>50</sub> values obtained against *P. falciparum* (*Pf*) and mammalian cell cultures.<sup>25,26</sup>

Herein, we characterized the activity of violacein against the different stages of the *Plasmodium* life cycle. Using chemical genomic profiling (CGP) to elucidate its mechanism of action, we found that violacein potentially affects the protein quality control system, more specifically, the Hsp90/Hsp70 interaction network. In order to investigate the effects of violacein on *Pf*Hsp90, structural and functional assays were performed. In addition, although there are six members of Hsp70 proteins in the *P. falciparum* genome, we selected *Pf*Hsp70-1 for all assays, due to its soluble nature when expressed *in vitro* and colocalization with its functional partner, *Pf*Hsp90.<sup>13,28,29</sup> Thus, we provide evidence that violacein is a dual chaperone binder that interacts with both *Pf*Hsp90 and *Pf*Hsp70-1 to increase protein unfolding and proteasome degradation. Additionally, the assays carried out with the *Saccharomyces cerevisiae* Hsp90 and Hsp70 proteins: ScHsp82 and ScSsa1, corroborate the idea that violacein can be capable of influencing the functions of these molecular chaperone families. Chaperone inhibition might shed light on violacein antitumoral, antipathogenic, and multistage antiplasmodial activities. The small molecule violacein may therefore provide a good scaffold for a chaperone-specific probe and/or for antimalarial drug design.

## 1. RESULTS

**1.1. Violacein Exhibits Multistage Antiplasmodial Activity.** Because violacein was previously shown to reduce parasitemia in mice infected with *Plasmodium*,<sup>27</sup> we aimed to

characterize the effect of this compound against other stages of the parasite's life cycle. To that end, we monitored the activity of violacein against asexual cultures of wild type (3D7) and multidrug resistant (Dd2 and W2) *P. falciparum* lines. Violacein displayed similar activity against all three strains, with an EC<sub>50</sub> ~ 400 nM (Figures 1A–C and Table S1). This finding suggests that the mechanism of action of and/or resistance to violacein is different to that of commonly used quinolone-based antimalarials.<sup>30–32</sup>

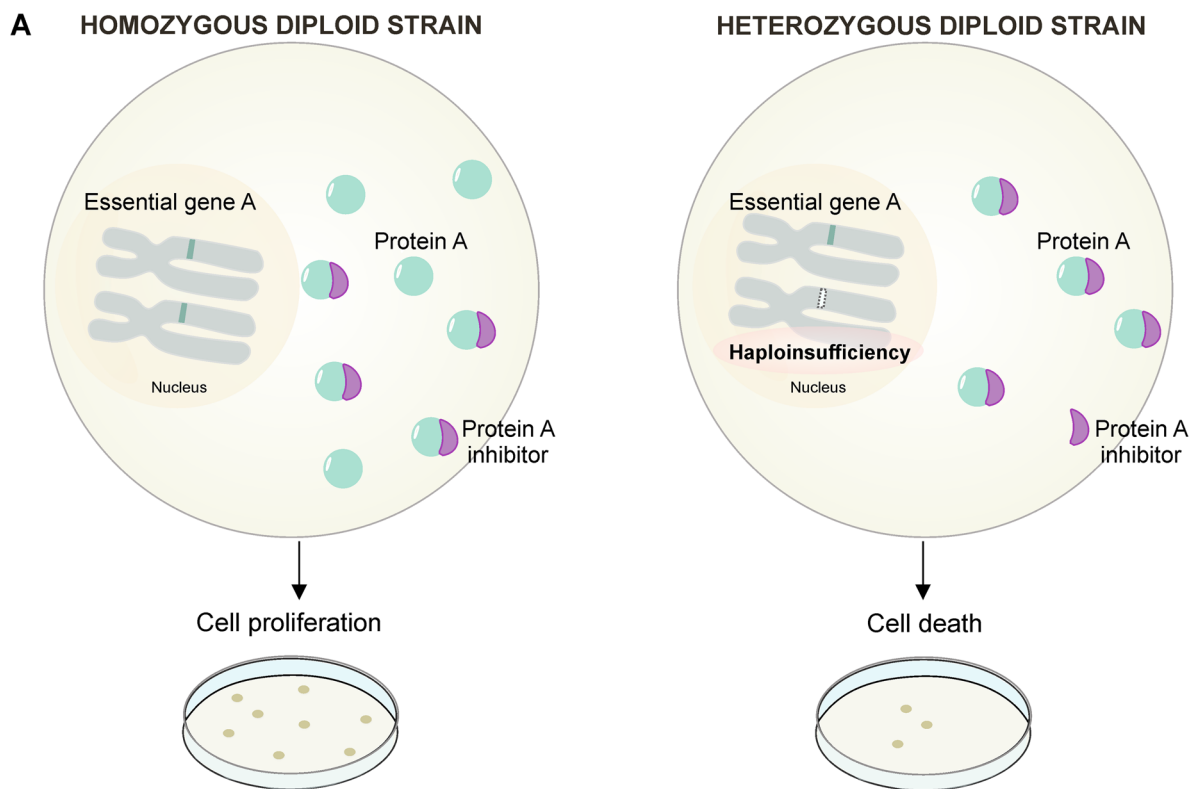
To determine the stage-specificity of action against asexual blood stages, we performed pulse treatments with violacein against highly synchronized parasite cultures at ring (young blood stage) or trophozoite (mature blood stage) stages, which revealed that violacein was most active against the mature asexual blood stages (Figure 1D). We next sought to investigate whether violacein exhibits fast or slow killing. We treated asynchronous parasite cultures with either violacein or control drugs known to exhibit fast (artesunate) or slow (pyrimethamine) killing activities. Consistent with a previous report,<sup>33</sup> violacein exerted a fast killing mechanism, with similar EC<sub>50</sub> values for three different incubation times (24, 48, and 72 h) (Figure 1E).

Strategies to prevent gametocyte uptake by mosquitos or to block parasite sexual stage development are essential to reduce the malaria burden.<sup>34</sup> Exposure to violacein for 48 h killed transmission-capable (stage V) gametocytes with an EC<sub>50</sub> value between 2.5 and 1.25 μM (Figure 1F). Furthermore, exposure to 2.5 μM of this compound completely removed gametocytes from the culture (data not shown).

Having shown that violacein has activity against both sexual and asexual blood stage parasites, we next performed standard membrane feeding assays (SMFAs) to determine the effect of violacein on mosquito stage parasites. We performed an SMFA whereby we exposed *Anopheles aquasalis* mosquitoes to a meal of blood from patients infected with *P. vivax* that had been incubated with violacein. At the minimum concentration tested (2.5 μM), violacein exhibited substantial insecticidal activity, killing 48% of the infected mosquitoes (Figure 1G and Table S1). Among the surviving mosquitoes treated with 2.5 μM violacein, there was a decrease of 17% in infection, and a significant decrease in oocyst numbers (43%) compared to the control group (Figure 1H, I and Table S1). It is possible that the reduction in sporogonic stages is a consequence of the gametocidal activity of violacein.

To determine whether violacein is active against liver stage parasites, we used a well-established luminescence-based *in vitro* infection system that employs human hepatoma cells infected with the rodent malaria parasite *P. berghei*.<sup>35</sup> Due to violacein toxicity to tumoral cells, we could not calculate the *P. berghei* EC<sub>50</sub>; however we could observe that, at 1 μM of violacein treatment, there was a reduction of hepatome infection of nearly 50%, without impairment in the liver cell (Figure 1J and Table S1). Furthermore, violacein affected cell confluency at concentrations >2 μM, which might be attributed to the antitumor properties of the compound. Taken together, violacein demonstrated a similar dose-range of activity against all the stages within the *Plasmodium* life cycle.

**1.2. Chaperone System Mutants Are Hypersensitive to Violacein.** CGP is based on the premise that diploid yeast containing a gene expressed in heterozygosis will become hypersensitive to sublethal doses of an inhibitor targeting the



**B**      Violacein vs Control (DMSO 0.5%)

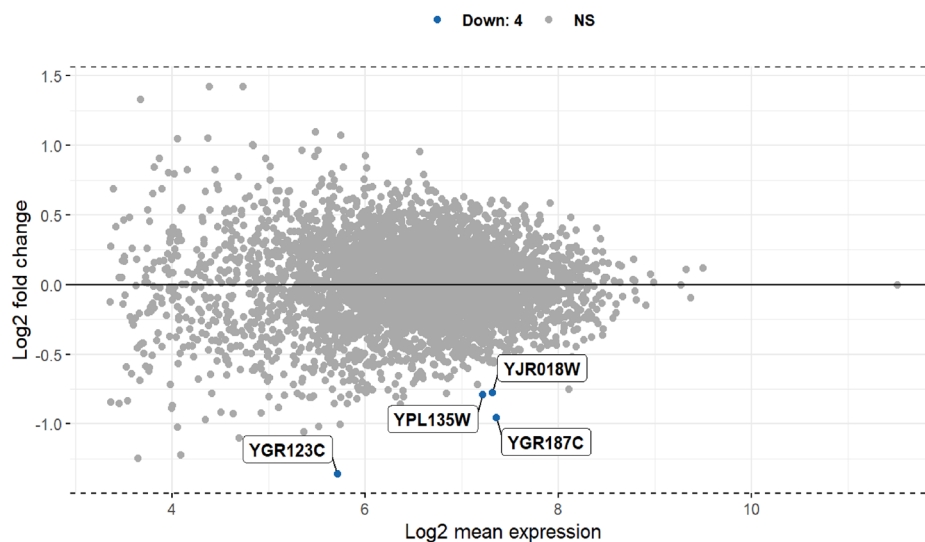


**Figure 2.** Violacein affects the chaperone system. (A) CGP works by comparing the growth of a pool of heterozygous diploid strains that was treated with a compound of interest with a pool treated with vehicle control, in a way to identify possible pathways targeted by the compound of study. As each mutant yeast strain carries a specific DNA-barcode, differential growth can be assessed by barcode sequencing. (B) Haploinsufficiency profile of heterozygous yeast pools treated with violacein. The log fold change is plotted on the y-axis as a function of the heterozygous yeast strains ordered alphabetically by their respective ORFs. The labels highlight the mutants that meet the condition of adjusted  $p$ -value < 0.01 and log<sub>2</sub> fold change < 0. The four hits labeled are yeast strains heterozygous for YGR123C (ScPpt1 protein), YGR187C (ScHgh1 protein), YPL135W (ScIsu protein), and YJR018W (dubious ORF).

product of this gene<sup>49–51</sup> (Figure 2A). This method has been previously used to identify drug targets in *Plasmodium*.<sup>40</sup>

Here, we used CGP to narrow down the mechanism of action of violacein. We cultured pools of ~6000 barcoded heterozygous yeast strains in the presence of violacein or

DMSO, extracted the genomic DNA, and performed deep barcode sequencing and barcode quantification. We then made comparisons in terms of the differential growth between yeast pools treated with violacein EC<sub>20</sub> or the equivalent concentration of vehicle control (Figure 2B). Usually in

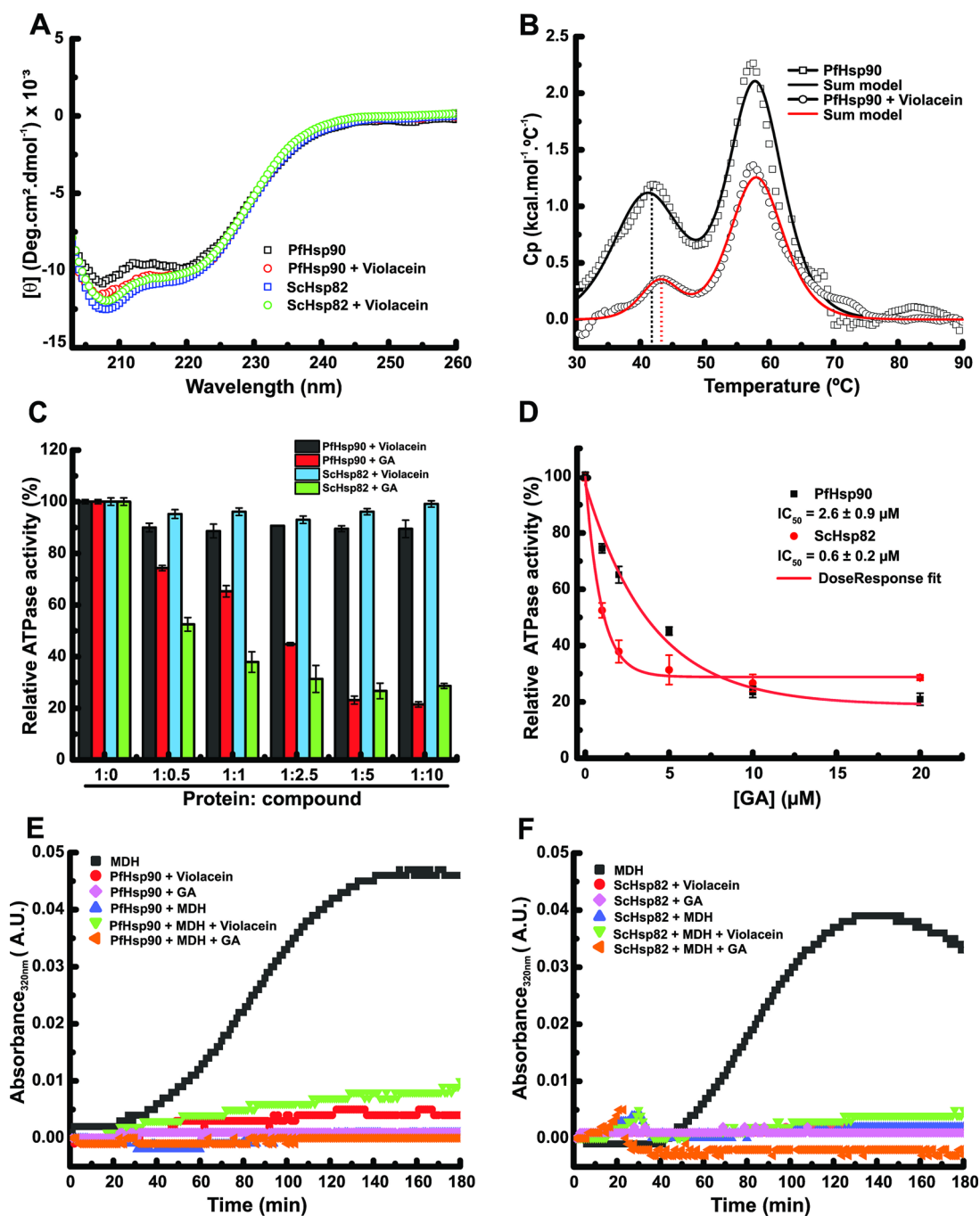


**Figure 3.** Violacein interactions with *PfHsp90* and *yHsp82* chaperones. (A) Structural changes in *PfHsp90* and *yHsp82* proteins in the presence of an equimolar concentration of violacein, determined by far-UV CD ( $n = 2$ ). (B) Thermal unfolding of *PfHsp90* in the presence of violacein, determined using DSC ( $n = 2$ ). The black and red dot lines highlight the differences in the first  $T_m$ , respectively, observed for the *PfHsp90* protein in the absence ( $T_{m1} = 41.0 \pm 0.2$  °C) and the presence of violacein ( $T_{m1} = 43 \pm 0.2$  °C) ( $n = 2$ ). (C) Bar graph of the relative ATPase activity of the *PfHsp90* and *yHsp82* proteins against different proportions of violacein and GA ( $n = 2$ ). (D) Relative ATPase activity assays for *PfHsp90* and *yHsp82* proteins as a function of GA concentrations. GA inhibited *PfHsp90* and *yHsp82* ATPase activity with  $IC_{50}$  values of  $2.6 \pm 0.9$  and  $0.6 \pm 0.2$   $\mu$ M, respectively. Dose–response fitting performed by OriginPro 2016 software ( $n = 2$ ). (E–F) Chaperone activity assays were performed using MDH protein as a model and an equimolar concentration of violacein and *PfHsp90* (E) or *yHsp82* (F). Black, blue, green, and orange symbols indicate MDH aggregation, MDH aggregation in the presence of *PfHsp90* or *yHsp82*, MDH aggregation in the presence of *PfHsp90* or *yHsp82* and violacein, MDH aggregation in the presence of *PfHsp90* or *yHsp82* and GA, and *PfHsp90* or *yHsp82* aggregation alone, respectively. The controls of the chaperones in the presence of violacein or GA are indicated by the red and lilac symbols, respectively ( $n = 2$ ).

chemical genomics using *S. cerevisiae*, heterozygous yeast pools are treated with  $EC_{20}$  concentration of a compound of interest for 20 generations.<sup>81</sup> In this work, we opted to treat the yeast pools with violacein  $EC_{20}$  concentration for 5 and 10 generations only, in a way to avoid false positives hits. This

decision came with the onus that statistics could be compromised, once the growth gap between yeasts with growth defects and nonaffected mutants were not as dramatic as they would be if they were set for 20 generations. For this reason, to find whether the drug treatment induces a change

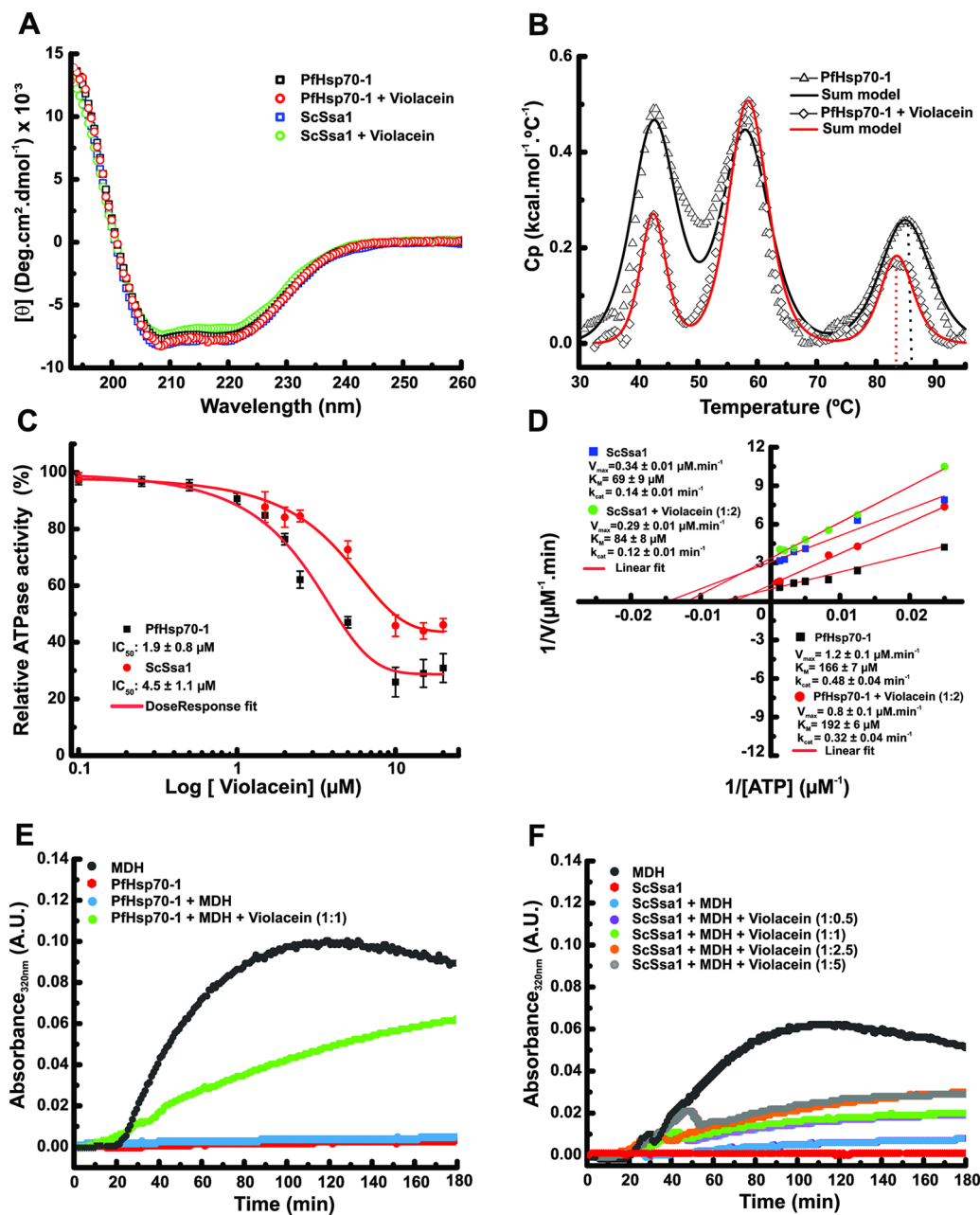


**Figure 4.** Violacein interactions with *PfHsp70-1* and SSA1 chaperones. (A) Structural changes in *PfHsp70-1* and SSA1 proteins in the presence of an equimolar concentration of violacein, determined by far-UV CD ( $n = 2$ ). (B) Thermal unfolding of *PfHsp70-1* in the presence of violacein, determined using DSC. The black and red dotted lines highlight the differences in the third  $T_m$  observed for the *PfHsp70-1* protein respectively in the absence ( $T_{m3} = 85.0 \pm 0.1$  °C) and presence of violacein ( $T_{m3} = 83.5 \pm 0.1$  °C) ( $n = 2$ ). (C) Relative ATPase activity for *PfHsp70-1* and SSA1 proteins in the presence of different violacein concentrations. The dose–response curves illustrate the inhibition profile, obtaining IC<sub>50</sub> values of  $1.9 \pm 0.8$  and  $4.5 \pm 1.1$  μM, respectively. Dose–response fitting performed by OriginPro 2016 software ( $n = 2$ ). (D) Lineweaver–Burk graphs for *PfHsp70-1* and SSA1 proteins ATPase activity in the absence and in the presence of violacein suggesting noncompetitive or mixed inhibition mechanism, abruptly changing the  $V_{max}$  values and smoothly altering  $K_M$ . (inset) Enzyme kinetic properties at each condition. The  $V_{max}$ ,  $K_M$  and  $k_{cat}$  values for *PfHsp70-1* in the absence of violacein were  $1.2 \pm 0.1$  μM/min,  $166 \pm 7$  μM, and  $0.48 \pm 0.04$  1/min. The  $V_{max}$ ,  $K_M$  and  $k_{cat}$  values for the *PfHsp70-1* in the presence of violacein (1:2) were  $0.8 \pm 0.1$  μM/min,  $192 \pm 6$  μM, and  $0.32 \pm 0.04$  1/min, respectively. The  $V_{max}$ ,  $K_M$  and  $k_{cat}$  values for the SSA1 in the absence of violacein were  $0.34 \pm 0.01$  μM/min,  $69 \pm 9$  μM, and  $0.14 \pm 0.01$  1/min. The  $V_{max}$ ,  $K_M$  and  $k_{cat}$  values for the SSA1 in the presence of violacein (1:2) were  $0.29 \pm 0.01$  μM/min,  $84 \pm 8$  μM, and  $0.12 \pm 0.01$  1/min, respectively. Enzyme kinetic properties at each condition estimated by linear fitting routine implemented by OriginPro 2016 software, accordingly to Lineweaver–Burk equation ( $n = 2$ ). (E) Chaperone activity assays were performed using MDH as a client protein model and an equimolar concentration of violacein and *PfHsp70-1*. Black, blue, green, and red symbols indicate MDH aggregation, MDH aggregation in the presence of *PfHsp70-1*, MDH aggregation in the presence of *PfHsp70-1* and violacein, and *PfHsp70-1* aggregation alone, respectively ( $n = 2$ ). (F) Assays for SSA1 chaperone activity were performed using MDH as a client protein model and different proportions of violacein. Black, blue, lilac, green, orange, gray, and red symbols indicate MDH aggregation, MDH aggregation in the presence of SSA1, MDH aggregation in the presence of SSA1 and violacein (1:0.5), MDH aggregation in the presence of SSA1 and violacein (1:1), MDH aggregation in the presence of SSA1 and violacein (1:2.5), MDH aggregation in the presence of SSA1 and violacein (1:5), and SSA1 aggregation alone, respectively ( $n = 2$ ).

in yeast abundance at any time point, we used an analysis design that included the generation as a regression variable and then tested using the likelihood ratio test where the generation factor was removed in the reduced formula (see [Data and Code Availability](#)).

The chemical genomic data did not highlight any enriched pathway or direct target of violacein. The small number of generations selected and the variability within replicates made it difficult to point with confidence the results of differential growth between vehicle and violacein treated pools. None of the four most significantly depleted yeast strains ( $\text{padj} < 0.01$  and  $\text{Log}_2$  Fold Change  $< 0$ ), were heterozygous for genes encoding essential proteins, but the two most significant depleted strains were heterozygous for genes coding chaperone related proteins: Hsp90 cochaperone protein (Ppt1/YGR123C) and chaperone protein (Hgh1/YGR187C), both with  $\text{padj} = 0.0011$ . Thus, we decided to use this information as a first indication to investigate if violacein is able to directly bind or functionally affect representatives of the three major chaperone families in *Plasmodium*: PfHsp90, PfHsp70, and PfTRiC.

**1.3. Violacein Binds PfHsp90, PfHsp70-1, ScHsp82, and ScSsa1 Molecular Chaperones.** Having shown that violacein might perturb chaperone function in yeast, we next investigated the capacity of violacein to bind and functionally affect PfHsp90, PfHsp70-1, and PfTRiC—three chaperones that are essential for *Plasmodium* survival.<sup>13,16,17,19</sup>

The binding of small molecules to a protein can change its circular dichroism (CD) spectrum profile due to chiral perturbations.<sup>41,42</sup> We thus used CD as an indicator of violacein–chaperone protein binding. Even low doses of violacein (1:1, PfHsp90:violacein) promoted slightly changes in PfHsp90 CD spectra ([Figure 3A](#)), suggesting an interaction between the two molecules. Similar findings were made for PfHsp70-1 ([Figure 3A](#)). Moreover, additional tests performed with the yeast Hsp90 and Hsp70 chaperones, ScHsp82 ([Figure 3A](#)) and ScSsa1 ([Figure 4A](#)) respectively, in the presence of equimolar concentrations of violacein, also suggest structural changes in these proteins caused by the interaction with violacein. We then used differential scanning calorimetry (DSC) to characterize the effects of violacein on chaperone protein unfolding and binding energetics. We performed DSC on full length PfHsp90 or PfHsp70-1, alone or preincubated with violacein ([Figures 3B](#) and [4B](#)). According to the literature,<sup>43,44</sup> the first PfHsp90 DSC peak corresponds to the N-terminal domain's melting point as it gains thermal stability in the presence of its natural binder, ADP, increasing the melting temperature peak 1 ( $T_{m1}$ ) up to 6 °C higher. Similar to ADP, violacein increased the PfHsp90 N-terminal domain melting temperature by  $\sim 2$  °C ([Figure 3B](#)) but not that of the C-terminal domain (second temperature transition) ([Table S2](#)). This indicates that violacein is able to thermally stabilize PfHsp90 nucleotide binding domain (NBD) but not the middle domain or C-terminal domain (PBD). The  $T_{m1}$  shift induced by violacein was accompanied by an increase in the total apparent enthalpy process ( $\Delta H1$ ), meaning that the energy required to complete the unfolding of the N-terminal domain was higher after violacein treatment. We obtained similar results in terms of subtle structural changes in PfHsp70-1 based on CD and DSC data ([Figure 4A](#) and [B](#)). The DSC tests indicate that the PfHsp70-1 interaction with violacein changed the third thermal denaturation transition ( $T_{m3}$ ) ([Table S2](#) and [Figure 4B](#)),

which is related to remaining structures from both Hsp70 domains<sup>45</sup> (NBD and PBD). This observation suggests that violacein can bind the interaction interface between the domains.

Finally, we analyzed whether violacein is able to affect *Plasmodium* CCT complex, or TRiC. A previous study suggested that TRiC regulation is involved in parasite resistance to the antimalarial drug, artemisinin.<sup>46</sup> Unlike PfHsp90 or PfHsp70-1, PfTRiC is a chaperonin complex formed by two rings composed by eight subunits each, which makes its expression in heterologous systems unviable. To assess the ability of violacein to interfere with *Plasmodium* TRiC, we compared the susceptibilities of knockdown parasites for TRiC to violacein treatment with that of their wild-type counterparts. There were no differences in the sensitivity to violacein between the knockdown parasites, and those expressing normal TRiC levels ([Figure S1](#)). These results indicate that PfTRiC activity is not compromised by violacein treatment.

In summary, our thermograph data reinforce the idea that violacein binds the PfHsp90 N-terminal domain (NBD), which comprises the chaperone ATP binding pocket and the PfHsp70-1 interface between NBD and C-terminal domains.

**1.4. Violacein Affects PfHsp70-1 and ScSsa1 ATPase Activity.** Because violacein is able to bind PfHsp90, PfHsp70-1, ScHsp82, and ScSsa1 chaperones, we monitored how violacein-mediated binding affects their ATPase activity. Natural products, such as geldanamycin (GA) and radiolol,<sup>47–49</sup> inhibit Hsp90 by competing with the nucleotide binding pocket at the N-terminal domain. Although there was no change in the ATPase activity of the PfHsp90 and ScHsp82 proteins in the presence of violacein ([Figure 3C](#)), in the presence of GA there was an inhibition of up to 70% of the ATPase activity of these proteins, which was also observed for other Hsp90.<sup>48,50</sup> The relative  $IC_{50}$  obtained for GA inhibition over PfHsp90 and ScHsp82 was  $2.6 \pm 0.9$  and  $0.6 \pm 0.2$   $\mu\text{M}$ , respectively ([Figure 3D](#)).

Although our biophysical assays performed in the presence of ADP suggested that violacein does not interfere with nucleotide binding ([Table S2](#)), we investigated the ATP turnover by PfHsp70-1 upon violacein treatment and used ScSsa1 for comparative purposes. The Hsp70 ATPase activity assays indicated a strong impairment on ATP hydrolysis ([Figure 4C](#)), with a relative  $IC_{50}$  value near the 1:1 molecular ratio of PfHsp70-1:violacein and 1:2 of ScSsa1:violacein, suggesting that the affinity between violacein and the plasmodial Hsp70 is greater than that of yeast, although they share 71% identity ([Figure S2](#)). Lineweaver–Burk ([Figure 4D](#)) and Michaelis–Menten ([Figure S3](#)) graphs of Hsp70 proteins in the presence of violacein (1:2 proportion of protein: compound) suggest that inhibition occurs through a noncompetitive or mixed mechanism, with a sudden change in the values of  $V_{\text{max}}$  and mild  $K_M$  ([Figures 4D](#) and [S2](#)). Thus, while violacein binding to PfHsp70-1 does not impair nucleotide binding, it significantly compromises ATP hydrolysis *in vitro*.

Hsp70 proteins exhibit a heterotropic bidirectional allosteric mechanism involved in client protein binding/releasing that is dependent on ATP hydrolysis and ADP exchange.<sup>51</sup> Changes in one domain may affect function of the other chaperone domain. Indeed, previous studies have highlighted the importance of PBD regulation for proper Hsp70 ATP hydrolysis.<sup>52–54</sup> In addition, the thermograms

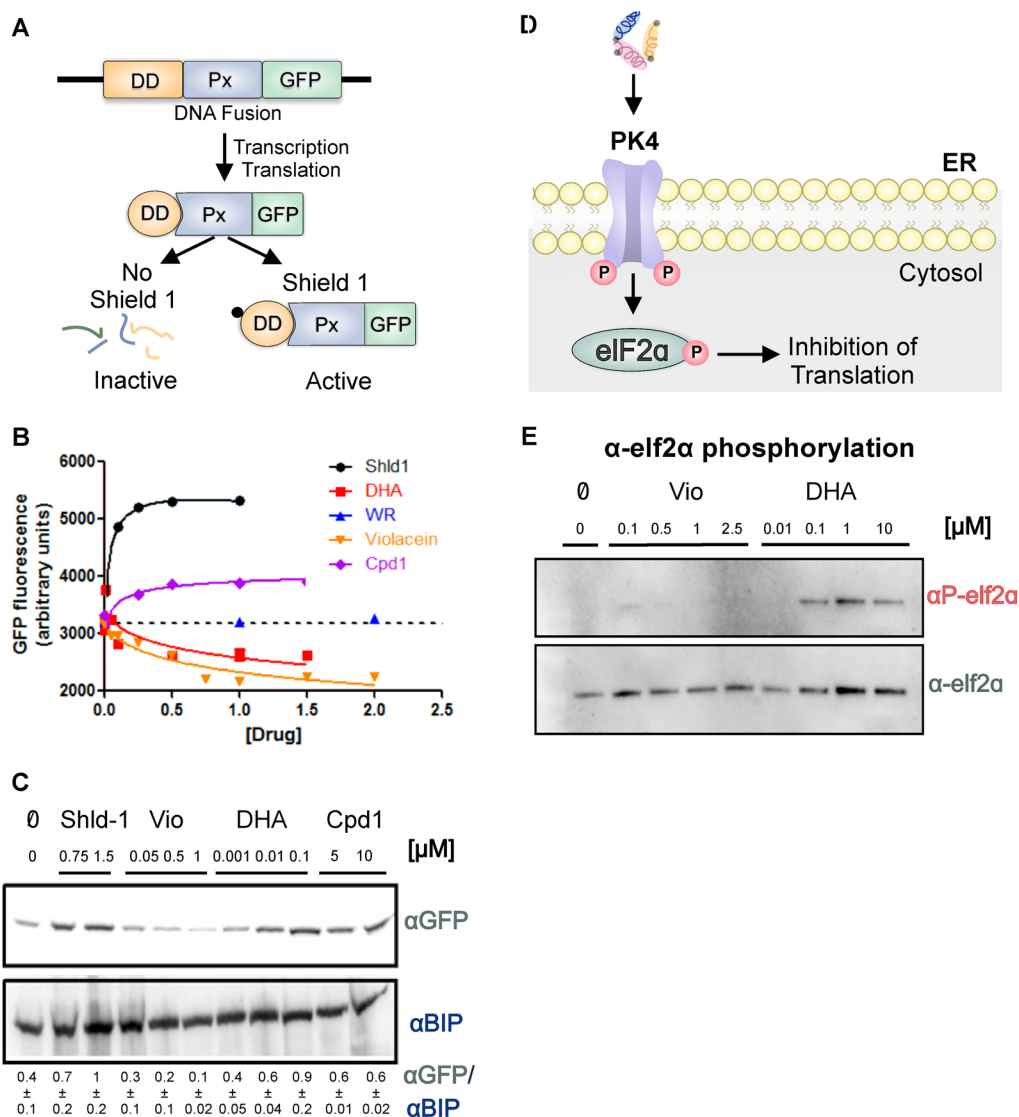


**Figure 5.** UPR and UPS response in *Plasmodium* upon violacein treatment. (A) *P. falciparum* 3D7-GFP-DD mutant parasite design. A gene encoding a destabilizing domain (DD) that is only stable in the presence of its ligand Shield-1, together with a GFP reporter gene (GFP) were attached to a protein known to be degraded by the *Plasmodium* proteasome (Px). In the presence of Shield-1, Px acquires a stable conformation and can be monitored by fluorescence via its GFP domain, while in the absence of Shield-1, Px gets unfolded due to the loss of the DD conformation and is targeted to proteasome degradation. (B) GFP fluorescence signals from mutant parasites are maintained in Shield-1 for 24 h before wash-out. Trophozoites were then treated for 3 h with compounds of interest: Shield (black), DHA (red), WR (blue), Cpd1 (purple), and violacein (orange) and fluorescence units were recorded by flow cytometry. Concentrations of Shield-1, violacein, DHA, and cpd1 are given in  $\mu\text{M}$ ; WR in  $\text{nM} \times 10$ . The dotted line represents background (sample fluorescence without Shield-1) ( $n = 3$ ). (C) The same mutant parasites analyzed in B were lysed, subjected to Western blotting, and probed with anti-GFP. The concentration ( $\mu\text{M}$ ) of compound used for the samples subjected to Western blotting is shown below the name of each compound. Anti-Bip was used as a loading control. Densitometry analysis (ImageJ) of the ratio between  $\alpha\text{GFP}/\alpha\text{Bip}$  (mean  $\pm$  SE) is shown in the gray box ( $n = 3$ ). (D) PK4 pathway activation in *Plasmodium*. Protein Kinase 4 (PK4) is an ER transmembrane protein that plays a major role in *Plasmodium* UPR. It is proposed that under ER stress conditions, unfolded peptides compete with PK4 for binding immunoglobulin protein (Bip) binding, causing the dissociation of Bip–PK4 interactions. Once no longer bound to Bip, it is suggested that the N-terminal domains of PK4 dimerize, inducing the autophosphorylation of the C-terminal eIF2 $\alpha$  kinase domain, followed by phosphorylation eIF2 $\alpha$ , which then leads to shut down in protein translation. (E) Western blotting against p-eIF2 $\alpha$ . NF54 parental line parasites were treated with different doses of violacein, DHA, or vehicle for 90 min at 37 °C, and parasite lysates were used for Western blotting. The concentration ( $\mu\text{M}$ ) of the compound used for Western blotting is shown below the name of each compound. Anti-eIF2 $\alpha$  was used as a loading control as indicated in the figure. ( $n = 2$ ).

obtained by the DSC (Figure 4B) corroborate the idea that violacein can bind in an interface region between the NBD and PBD, indirectly influencing hydrolysis. Taken together, violacein potentially disturbs the ATPase activity of Hsp70 chaperones studied here, which is essential for the functional cycle of these chaperones.

**1.5. Violacein Compromises Hsp70 Chaperone Function in Preventing Protein Aggregation.** One of the key functions of Hsp90 and Hsp70 molecular chaperones is to assist with protein maturation and prevent the aggregation of misfolded protein intermediates.<sup>55</sup> Unlike Hsp70 proteins that have a specific region that interacts with client substrates to prevent protein aggregation, Hsp90

has several binding sites for client proteins along its dimeric structure.<sup>56</sup> In this sense, we evaluated whether chaperone–violacein interactions could disturb the capacity of *PfHsp90*, *PfHsp70-1*, *ScHsp82*, and *ScSsa1* to prevent thermally induced aggregation of malate dehydrogenase (MDH) *in vitro*.

Violacein treatment did not impair the ability of *PfHsp90* and *ScHsp82* to prevent aggregation of MDH (Figure 3E and F). The same was observed for *Hsp90* in the presence of GA, which suggests that the binding of this inhibitor in the *Hsp90* N-terminal domain does not affect the chaperone ability to prevent protein aggregation *in vitro*. A study by Kravats and colleagues<sup>57</sup> showed that the presence of GA interferes with the formation of the yeast protein complex *Hsp82-Ssa1-Sis1-Sti1* and consequently decreases the efficiency in reactivation of heat-inactivated luciferase by this protein system. These data suggest that, although the role of *PfHsp90* and *ScHsp82* proteins in preventing aggregation is not impaired in the presence of GA, refolding of client proteins assisted by *Hsp90* may be affected. On the other hand, treatment with violacein in equimolar doses impaired the chaperone function of the *PfHsp70-1* (~70%) and *ScSsa1* (~30%) proteins, respectively (Figure 4E, F and Table S4), showing a stronger effect on *P. falciparum* *Hsp70* than on the *S. cerevisiae* counterpart. Moreover, the increase in the proportions of violacein resulted in a decrease in the ability of *ScSsa1* to prevent the aggregation of MDH (Figure 4F and Table S3), which suggests a dose-dependent action. This finding is consistent with our earlier results showing that violacein modifies the *Hsp70-1* C-terminal domain or neighboring regions of the PBD (Figure 4B), as *Hsp70* chaperones prevent protein aggregation by sequestering client proteins with exposed hydrophobic regions via the PBD.<sup>55</sup> Most *Hsp70* inhibitors interact with the NBD, impairing ATP binding.<sup>58,59</sup> Here, we describe a different mechanism of inhibition via the interface region between the NBD and PBD domains, suggesting that the interdomain communication is important for both *PfHsp70-1* ATP hydrolysis and chaperone activity.

**1.6. Violacein Causes Protein Degradation via Proteasome.** The ubiquitin proteasome system (UPS) and unfolded protein response (UPR) form two major regulatory branches of cell stress signaling in which chaperones have a pivotal role.<sup>15,60</sup> To evaluate if violacein is causing protein unfolding and/or proteasome degradation in *Plasmodium*, we used mutant parasites expressing a GFP reporter linked to a destabilizing domain (DD), which is only stable in the presence of a binding ligand, Shield-1. In the absence of Shield-1, the destabilized protein is turned over rapidly by the proteasome and the fluorescence signal is decreased; while in the presence of Shield-1, the fluorescence signal increases due to accumulation of the GFP domain (Figure 5A).<sup>61,62</sup> Parasites treated with violacein were compared to five control groups treated with the following molecules: Shield1; Compound 1 (Cpd1), a pan-inhibitor of ubiquitin-activating enzymes (E1); dihydroartemisinin (DHA), the gold standard antimalarial known to cause promiscuous protein damage/unfolding and also partial inhibition of the proteasome; and WR99210, an antifolate antimalarial that does not affect UPS in *Plasmodium*. Folded proteins were detected by flow cytometry (FC) through GFP fluorescence signals, while the total amount of protein was obtained by Western blotting (WB), using antibodies against GFP. As expected, in mutant parasites treated with compounds known to impair proteasome degradation, such as Cpd1 and DHA, proteins

are not degraded (as shown in WB data, Figure 5C).<sup>61</sup> The gain of GFP signaling in FC presented by *cdp1* treated parasites is consistent with accumulation of proteasome substrate that is not recognized/degraded, as it is not ubiquitinated. For DHA treated parasites, despite the accumulation of mutant proteins observed by WB, the GFP signal is below the background control line (presented by WR99210 and nontreated parasites). This was expected as DHA causes protein unfolding, and the lack of signaling might be due to DHA-induced loss of GFP native conformation. Violacein showed decreased signaling for both, GFP fluorescence and total amount of GFP, indicating that proteins are being unfolded and subsequently degraded by the proteasome (Figure 5B and C).

**1.7. Violacein Does Not Activate Plasmodium Unfolded Protein Response.** While in mammalian systems, we have a robust UPR response composed by three majoritarian arms, IRE-1, PERK, and ATF6, in *Plasmodium* this response is reduced to a modified PERK pathway that lacks transcriptional regulatory response. Under accumulation of misfolded proteins, BiP dissociates from PK4, a transmembrane kinase that undergoes autophosphorylation prior to phosphorylation of eIF2 $\alpha$ , resulting in protein translation shut down, in a way to avoid chaperone overload<sup>63</sup> (Figure 5D). Thus, we can say in that *Plasmodium*, eIF2- $\alpha$  phosphorylation implies in decreased protein translation,<sup>63</sup> indicating UPR activation<sup>15,60</sup> (Figure 5D). We investigated the profiles of eIF2- $\alpha$  phosphorylation in parasites treated with violacein. As previously reported,<sup>61</sup> DHA treatment activates parasite UPR by promoting shut-down in protein translation via eIF2- $\alpha$  phosphorylation as a consequence of the buildup of polyubiquitinated proteins. Violacein treatment did not result in eIF2 $\alpha$  phosphorylation (Figure 5E), suggesting that protein synthesis is not hampered by UPR activation (for biological replicate see Figure S4). Altogether, this data indicates that violacein is not causing accumulation of unfolded proteins in *Plasmodium* parasites, which is in accordance with our previous data showing that misfolded proteins are likely being degraded by the proteasome (Figure 5B and C).

## 2. DISCUSSION

Violacein is a naturally occurring small molecule that has the ability to control malaria in mice.<sup>27</sup> There are hundreds of studies reporting the activity against different organisms and models, such as bacteria, viruses, and cancer cells. In this work, we tested violacein activity against three different *Plasmodium* species in a way to cover the life cycle of *Plasmodium* spp. We used the widespread *P. berghei* murine model, to evaluate the activity of violacein against liver stage parasites. Using *P. berghei* as a model has some advantages over *P. falciparum* when performing drug screening against hepatic stages, as it poses lower biosafety risks, generates more sporozoites, has a shorter cycle within hepatocytes, and can easily infect hepatoma cell lines.<sup>64</sup> *P. vivax* and *P. falciparum* are the major *Plasmodium* species responsible for malaria burden in humans, thus the principal targets for therapeutic intervention. Due to the lack of a continuous *in vitro* culture,<sup>65</sup> usually *P. vivax* is excluded from the malarial drug discovery pipeline, which is focused mainly in *P. falciparum*. Here, we performed a standard membrane feeding assay (SMFA) using *P. vivax* field isolates to evaluate if violacein impairs transmission in this model. Finding compounds that are able to block *P. vivax* transmission has an epidemiologic

importance in *P. vivax* control, once one of the main reasons that underlies the difficulty in blocking *P. vivax* transmission happens due to its ability to produce gametocytes at the very beginning of infection, contributing to high transmission rates.<sup>66</sup>

To guide our investigations on the mode of action of violacein, we performed yeast-based chemical genomic profiling, an assay that allows us to identify from a pool of mutants, the heterozygous yeast strains that are most sensitive to violacein, giving us a clue about possible targets or biochemical pathways affected by the compound. Although we did not obtain clear targeted pathways or proteins in our CGP screen, the fact that two out of four hits are involved in chaperone processes made us hypothesize that violacein might be interfering with the chaperone system. Thus, we decided to investigate whether violacein could indeed be affecting this protein quality control network by investigating the interaction of violacein with the yeast Hsp90 and Hsp70 chaperones, (ScHsp82 and ScSsa1, respectively) and with the three major components of the parasite's chaperone system: PfHsp90, PfTRiC, and PfHsp70-1.

We found that violacein binds the two most abundant chaperones in *Plasmodium*, PfHsp90 and PfHsp70-1,<sup>12</sup> which are known to be active in proteostasis when they work together.<sup>28,67</sup> We found no evidence of an interaction of violacein with PfTRiC. Although violacein treatment does not interfere with the ATPase activity of PfHsp90, it impairs PfHsp70-1 ATP hydrolysis. In addition to compromising nucleotide exchange, violacein binding to the PfHsp70-1 PBD/NBD inhibits its chaperone function *in vitro*. Violacein was also shown to bind the yeast functional partners ScHsp82 and ScSsa1,<sup>57</sup> inhibit the ATPase activity of ScSsa1 and to impair its chaperone activity in a similar fashion as it does for the *Plasmodium* ortholog, PfHsp70-1.

A recent study showed that violacein induces aggregation of actin in *Plasmodium* without affecting actin polymerization.<sup>68</sup> The study suggests that violacein might be interacting with actin indirectly via actin binding partners or by disturbing the *Plasmodium* foldosome, in which Hsp70 and Hsp90 are critical players for the surveillance of protein folding, trafficking, quality control, and degradation processes.

To investigate if violacein affects the ubiquitin proteasome system in *Plasmodium*, we used *P. falciparum* parasites transfected with plasmids containing a modified PFKBP gene, which codes a protein known to be quickly degraded by the proteasome attached to a destabilizing domain (DD) (only stable in the presence of its ligand Shield-1) and a GFP reporter gene. Although we did not performed a direct assay showing violacein interaction with proteasome, the diminished values of GFP signaling and total amount of protein, observed by both, FC and WB, supports the idea that violacein does not impair proteasomal degradation, as the experiment suggests that violacein causes protein unfolding followed by intense protein degradation via proteasome. Because UPR in *Plasmodium* is triggered by accumulation of unfolded proteins, it is not surprising that, in violacein treated parasites, this branch of the stress response is not activated (no phosphorylation of eIF2- $\alpha$ ). Thus, these experiments suggest that violacein is causing protein unfolding/degradation, but protein synthesis does not seem to be discontinued as a result of UPR stress response activation. In summary, our data indicates that the system for attenuating protein synthesis is

not disrupted, permitting ongoing protein synthesis. However, protein synthesis itself is an error-prone process that heavily relies on chaperones to succeed, supporting violacein-induced collapse of proteostasis (Figure 6).

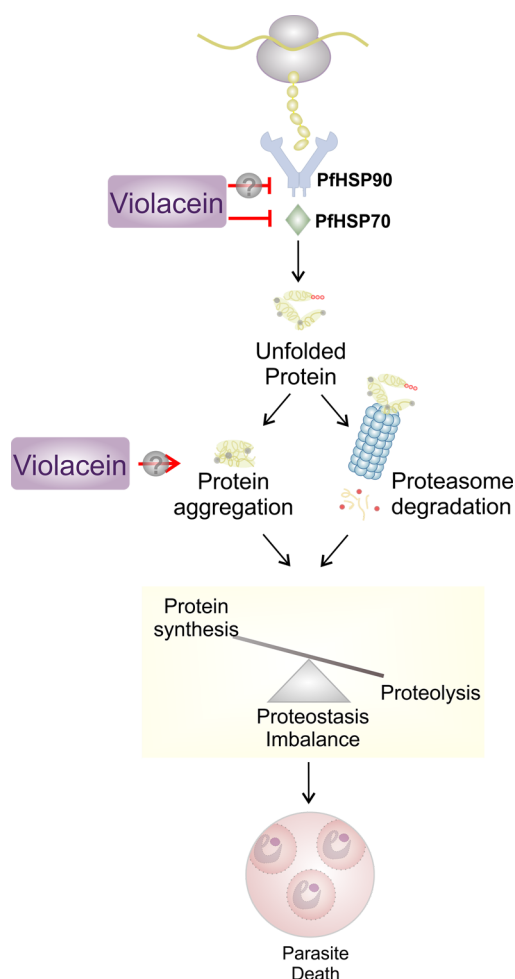


**Figure 6.** Proposed mechanism for violacein mode-of-action in *Plasmodium*. Violacein promotes PfHsp70-1 inhibition with possible impairment on PfHsp90 chaperone activity, preventing folding of damaged and newly synthesized peptides. Chaperone overburden shifts its function toward proteolytic pathways, culminating in protein polyubiquitination and intense proteasome degradation that leads to imbalanced proteostasis, causing parasite death. Despite intense proteolysis, protein synthesis continues, possibly in an attempt to compensate for the loss of essential proteins by the proteasome, reinforcing violacein-induced proteostasis collapse.

Importantly, the results presented here do not sustain the idea that the Hsp90/70 network is the only target of violacein. It is possible that violacein is a promiscuous compound that causes protein damage as a whole, and the loss of function of the chaperone network reinforces the proteostasis collapse causing cellular death.

Chaperones were first proposed as drug targets in the early 1990s, for cancer therapeutics. Two decades later, there were already 17 inhibitors at clinical trials, making chaperones one of the most pursuit targets for oncological treatment in earlier 21st century.<sup>69</sup> Nonetheless, clinical use of these molecules have been hampered by toxicity.<sup>70</sup> As is the case for proteasome inhibitors, chaperone inhibitors might face obstacles regarding compound selectivity for the parasite

target, due to high rates of conservation of chaperones. Going forward, as violacein potential to bind PfHsp70-1's interface between NBD and PBD, a variable domain within human and parasite chaperones, makes it a scaffold to be considered for future probe for molecular chaperone network or/and antiplasmodial drug design approaches. We anticipate that due to the high degree of protein conservation, chaperone inhibition might shed light on antitumoral, antipathogenic, and multistage antiplasmodial activities of violacein.

### 3. CONCLUSION

Despite advances in understanding of evolution, genetics, and proteomics of different organisms, our comprehension on how small molecules evolved to control these processes falls short. Natural products are an important source of therapeutic chemical scaffolds and, historically, have played an important role in malaria chemotherapy. Here we show that the naturally occurring molecule, violacein, is able to bind the functional partners, Hsp90 and Hsp70-1, the two most abundant *P. falciparum* chaperones. This binding compromises the ATPase activity of PfHsp70-1 and the chaperone function in preventing protein aggregation is greatly impaired *in vitro*. Inhibition of the chaperone system is consistent with observed changes in protein folding and proteasome degradation in violacein-treated *P. falciparum* and might underline the multistage antiplasmodial properties of violacein. The use of unbiased methods for target fishing in *P. falciparum*, such as genome-wide thermal proteome profiling or genomic analysis of violacein-resistant lines, are important for further validation of the present findings.

### 4. METHODS

**4.1. Experimental Models.** **4.1.2. *P. falciparum* Culturing.** The *P. falciparum* chloroquine-sensitive strains (3D7), multidrug resistant strains (W2 and Dd2), and the mutant strain, GFP-DD, used in this study were cultured at 4% hematocrit in type O+ human red blood cells (Hematology Center of University of Campinas) and maintained at 37 °C in an atmosphere containing 1% O<sub>2</sub>, 5% CO<sub>2</sub>, and 94% N<sub>2</sub> in RPMI medium supplemented with 10% pooled human serum (Hematology Center of University of Campinas).<sup>71</sup>

**4.1.3. Huh7 Cell Culturing.** Huh7 cells were routinely cultured in RPMI 1640 medium supplemented with 10% (v/v) fetal bovine serum, 1% (v/v) glutamine, 1% (v/v) penicillin/streptomycin, 1% (v/v) nonessential amino acids, and 10 mM HEPES, and incubated at 37 °C in a humidified atmosphere containing 5% CO<sub>2</sub>.

**4.1.4. Mosquito Rearing and Parasite Production.** All animal experiments were performed in strict compliance with the guidelines of the animal ethics committee of Instituto de Medicina Molecular João Lobo Antunes (iMM JLA, Lisboa, Portugal) and the Federation of European Laboratory Animal Science Associations (FELASA). Animals were purchased from Charles River Laboratories and kept under specific pathogen-free conditions in iMM JLA's animal facility.

BALB/c mice were infected by intraperitoneal (i.p.) injection of RBCs infected with luciferase (Luc)-expressing *P. berghei* ANKA parasites.<sup>72</sup> Female *Anopheles stephensi* mosquitoes, reared at iMM JLA, were fed on the infected mice for sporozoite production. Following infection, mosquitoes were maintained at 20 °C and 80% humidity and were fed on 5% (w/v) glucose and 0.05% (w/v) PABA solution.

**4.1.5. Patient Blood Samples.** Blood samples were collected from six individuals infected with *P. vivax* (with parasitemia  $\geq 2\%$ ). All participants provided a signed Informed Consent Form. The project was approved by the Research Ethics Committee (no. 2.584969 of April 6, 2018). Patient blood (~5 mL) was collected by venipuncture, and the samples were placed into a sterile heparinized vacutainer tube in the Fundação de Medicina Tropical Doutor Heitor Vieira Dourado (FMT-HVD) (Manaus, Amazonas, Brazil).

**4.1.6. *Anopheles aquasalis* Maintenance.** *Anopheles aquasalis* were reared at the insectaries of the Laboratory of Medical Entomology at the FMT-HVD. Colonies were kept at a 24–26 °C and a relative humidity of 70–80% on a 12:12 light–dark cycle. Larvae were hatched at room temperature, in water containing salt at a final concentration of 2 g/L, and ground fish food (Tetramin Gold) was provided daily. Larvae were allowed to pupate and become adults in an enclosed mesh-covered cage with water and fed *ad libitum* with a 10% sucrose solution until 2 d before being given the infective blood meal.<sup>73</sup>

**4.1.7. Yeast Cultures.** Wild type yeast (BY4743) was cultured in complete YPD (1% w/v yeast extract; 2% w/v peptone; 2% w/v glucose) at 30 °C and 200 rpm. Heterozygous mutant yeast pool was maintained and cultured in complete YNB (YNB drop-out minus uracil; 2% w/v glucose, 2% uracil) at 30 °C and 200 rpm.

**4.2. Methods Details.** **4.2.1. Chemicals.** Violacein was purchased from Sigma-Aldrich (Janthinobacterium lividum V9389) or produced in an *E. coli* heterologous system.<sup>25</sup> The compound obtained from either source has a minimum purity of 85%.

**4.2.2. Inhibitory Concentration Assay against *P. falciparum* Asexual Stages.** Drug inhibition assays were performed as previously described.<sup>74</sup> Briefly, D-sorbitol synchronized ring cultures (0.5% parasitemia and 2% hematocrit) were plated in 96-well plates in the presence of different concentrations of violacein or of the drug vehicle (DMSO), as a control. After 72 h of incubation, parasitemia was assessed by fluorometry using SybrGreen (see table of resources) fluorescent dye. EC<sub>50</sub> values were calculated by plotting Log dosing vs growth inhibition (expressed as percentage relative to the drug-free control).

**4.2.3. Violacein Stage Specificity within *P. falciparum* Asexual Parasites.** Hyper-synchronized 3D7 schizonts were enriched by incubating the parasite culture with two rounds of 5% sorbitol followed by 65% Percoll purification. Schizonts were collected and reincubated for 3 h to allow merozoite egress and reinvasion. After incubation for 0–3 h or 20–23 h, the parasite culture was again sorbitol-synchronized for early ring or trophozoite stage purification. Highly synchronized ring-stage parasites were plated in a 96-well plate following the same adjustments and treatments as described in section 4.2.2. For ring stage susceptibility, parasites purified 0–3 h postinvasion were incubated with the indicated compounds of interest for 18 h. For trophozoite stage susceptibility, parasites purified 20–23 h postinvasion were treated with the indicated compounds of interest and controls for 18 h. Parasitemia and EC<sub>50</sub> values were calculated as described in section 4.2.2.

**4.2.4. Violacein Speed of Action.** The speed of violacein action was evaluated as previously described.<sup>33</sup> Briefly, parasite growth was evaluated departing from an asynchronous culture in the presence of violacein and control antimalarial

compounds: artesunate (quick action) and pyrimethamine (slow action).<sup>33</sup> *P. falciparum* 3D7 parasites were incubated in the same conditions as described in 5.2.2, with the exception that the parasites were treated for 24, 48, and 72 h (the standard time for this assay) with the compounds of interest and subsequently frozen for 24 h at  $-20^{\circ}\text{C}$ . Data were acquired by fluorometry according to the SybrGreen protocol, as described in in section 4.2.2.

**4.2.5. Violacein Activity against Hepatic Infection by *P. berghei*.** Hepatic stage susceptibility assays were performed as previously described.<sup>72</sup> Briefly, Huh7 cells were seeded on a 96-well plate at  $1 \times 10^4$  cells/well in 100  $\mu\text{L}$  of culture medium, RPMI medium supplemented as described in in section 4.2, and incubated overnight at  $37^{\circ}\text{C}$  in a humidified atmosphere containing 5%  $\text{CO}_2$ . The cells were then incubated with vehicle drug control (DMSO) or with different concentrations of violacein diluted in infection medium, i.e. culture medium supplemented with gentamicin (50  $\mu\text{g}/\text{mL}$ ) and amphotericin B (0.8  $\mu\text{g}/\text{mL}$ ), in triplicate wells. Firefly luciferase-expressing *P. berghei* sporozoites were obtained from dissected salivary glands of infected female *Anopheles stephensi* mosquitoes. Then,  $1 \times 10^4$  sporozoites were added to which well, and the plates were centrifuged for 5 min at 1800g prior to incubation for 46 h at  $37^{\circ}\text{C}$  in 5%  $\text{CO}_2$ .

Compound cytotoxicity was assessed by measuring cell confluency. Here, the culture medium was removed from the plate and 80  $\mu\text{L}$  of a 1:20 solution of AlamarBlue prepared in complete RPMI medium was added to each well and incubated for 1.5 h at  $37^{\circ}\text{C}$  in 5%  $\text{CO}_2$ . Fluorescence was measured on a plate reader at 530 nm excitation and 590 nm emission wavelengths. Infection rates were assessed by luminescence reading following cell lysis and addition of the luciferin substrate (Biotium, USA). Briefly, the AlamarBlue solution was removed and each well was washed with PBS. Then, cell lysis buffer (70  $\mu\text{L}/\text{well}$ ) was added to each well and incubated for 15 min at room temperature, with shaking at 600 rpm. The plates were then centrifuged for 5 min at 1800g to remove the cell debris/membranes, and 30  $\mu\text{L}$  of the lysed supernatant was transferred to a 96-well nucleon flat white plate, followed by the subsequent addition of 50  $\mu\text{L}/\text{well}$  luciferin solution.

**4.2.6. Violacein Activity against *P. falciparum* Gametocytes.** The high producing gametocyte NF54-Luc strain was cultured following standard culture procedures, as described in in section 4.2. Gametocytes were produced as previously described.<sup>75,76</sup> Briefly, parasites were cultured until they reached 8–10% parasitemia at trophozoite stages. Parasite culture containing spent medium was resuspended and transferred to a T-175 flask containing complete parasite medium (3/4 volume of the culture), and hematocrit was adjusted to 5%. The culture was maintained for 10 days in the presence of 62.5 mM *N*-acetyl glucosamine to inhibit merozoite invasion and thus asexual replication. The medium was changed daily without addition of RBCs. To evaluate whether violacein can affect gametocyte stage V viability, stage V NF54-Luc gametocytes were magnet-purified and treated with violacein for 48 h at 2% gametocytemia and 1.5% hematocrit in a gas chamber at  $37^{\circ}\text{C}$  prior to luciferase activity measurements. Luciferase activity was determined in 20  $\mu\text{L}$  parasite lysates by adding 50  $\mu\text{M}$  of luciferin substrate (Promega Luciferase Assay System) at room temperature (RT) and detection of resultant bioluminescence at an

integration constant of 10 s with the GloMax-Multi+ Detection System with Instinct Software.

**4.2.7. *Anopheles aquasalis* Oocyst Density Evaluation by Standard Membrane-Feeding Assay (SMFA).** For *An. aquasalis* infection, blood from *P. vivax*-infected patients was centrifuged at 500g and resuspended in 40% hematocrit with AB+ plasma and violacein or vehicle control (DMSO) was added. Mosquitoes were divided into experimental groups (violacein in 2.5, 5, and 10  $\mu\text{M}$  diluted in DMSO) and a control group (blood plus 0.1% DMSO) and exposed for 2 h to a blood meal. Seven days postinfection, the midguts were dissected in PBS, placed on a glass slide, and stained with 0.1% commercial Mercurochrome (Merbromin, Saint Louis, USA). The infection rate (percentage of infected midguts) and the infection intensity (mean number of oocysts/midgut) on each mosquito were recorded and compared.

**4.2.8. CGP Using the Yeast Model.** A collection of  $\sim 6000$  yeast strains was collected, where one copy of each of the predicted *S. cerevisiae* open reading frames (ORFs) was replaced by an antibiotic resistance marker (KANMX4). Each cassette was flanked by 20-bp DNA barcode sequences unique to each of the deleted ORFs, as described previously.<sup>36–39,77,78</sup> These barcodes were flanked by sequences allowing amplification of all “uptags” and “downtags” by common primer pairs. The violacein  $\text{EC}_{20}$  was determined for wild-type yeast (BY4743), as previously described.<sup>79</sup> The heterozygous yeast pool collection was distributed in 500  $\mu\text{L}$  YNB complete medium in triplicates, either with violacein  $\text{EC}_{20}$  or vehicle control in 48-well plates kept at  $30^{\circ}\text{C}$  with agitation at 200 rpm. A fraction (1/20) of the culture was diluted in a new plate every 12 h for 24 h (5 and 10 yeast generations). Cultures were harvested by centrifugation and were resuspended on TE buffer and stored at  $-80^{\circ}\text{C}$  until further use.

Genomic DNA was extracted using a Wizard Genomic DNA Purification Kit (Promega), according to the manufacturer's conditions. Purified genomic DNA was sent for barcode sequencing at the Centro de Sequenciamento Genômico da Universidade de São Paulo/ESALQ. Data obtained from Illumina sequencing (100 bp paired-end reads) were subsequently processed for barcode quantification. Briefly, the DESeq2 package (version 1.30.0) was used to normalize the barcodes counts and to estimate the differential abundance between treated samples and their respective controls.<sup>80</sup> A filter was further established to remove the barcodes with a low count along the samples (<10 observations in six samples). Differentially depleted barcodes were identified using a maximum likelihood ratio test (LRT), which consists of a generalized linear model in which the number of observations of a given barcode is described by a negative binomial distribution whose average is given by the treatment. Normalization between samples was achieved by library size factor method, using only amplicon sequence variants (ASVs) with the number of observations > 0. We considered significant hits strains that presented an adjusted *p*-value < 0.01 and log<sub>2</sub> fold change < 0 (growth defect). For more information and details for code reproducibility, please see [Data and Code Availability](#).

**4.2.9. Cell Lysate Analysis by Western Blotting.** Protein lysates for Western blotting were prepared from a Pf3D7 culture of 5% trophozoite at 5% hematocrit treated with different concentrations of compounds, as indicated in the figure legends, for 3 h at  $37^{\circ}\text{C}$ , as previously described.<sup>61,62</sup>

For experiments using GFP-DD mutant parasites, 5% trophozoite culture at 5% hematocrit was subjected to different compound treatments for 3 h. Parasites were then isolated with 0.05% (w/v) saponin and the pellet was washed three times with PBS supplemented with an EDTA-free protease inhibitor cocktail (Roche). Parasite pellets were next solubilized in SDS-PAGE loading buffer and separated on a 4–12% Bis-Tris acrylamide gel (Life-Technologies) using MES or MOPS running buffer and transferred to a nitrocellulose membrane (iBlot; Life Technologies).<sup>61</sup> After blocking, the membranes were probed overnight at 4 °C with the following primary antibodies: mouse anti-GFP (Roche; 1:1000), mouse anti-Pf-BiP (1:1000), rabbit antiphospho-eIF2- $\alpha$  (Cell signaling Technology; 1:1000). After washing with TBS-T, the membranes were probed with the following secondary antibodies: goat antirabbit IgG-peroxidase (Sigma-Aldrich-A0545; 1:20,000) and goat antimouse IgG-peroxidase (Chemicon-AP127P; 1:20,000). The membranes were then washed with TBS-T and incubated with enhanced chemiluminescent (ECL) reagents (Bio-Rad), prior to chemiluminescence detection employing a Bio-Rad ChemiDoc MP imaging system.

**4.2.10. GFP Fluorescence Measurement Using Flow Cytometry.** Cultures of GFP-DD mutant parasites with 5% trophozoite at 5% hematocrit were exposed to the indicated drug treatments for 3 h. Parasite samples were stained with 2  $\mu$ M SYTO-61 for 20 min and adjusted to 0.1% hematocrit in PBS for plate reading using a FACSCantoTM II cytometer (Becton Dickinson). The data were analyzed using FlowJo (version 10) software, with the parasites gated based on the SYTO-61 signal. The GFP fluorescence of the parasites was reported as the fluorescence values. Data were fit by nonlinear regression and plotted using GraphPad Prism software.

**4.2.11. Recombinant Protein Expression, Purification and Bioinformatics Analysis.** Recombinant PfHsp90 (XP\_001348998.1), PfHsp70-1 (XP\_001349336), and ScHsp82 (NP\_015084.1) proteins were expressed by the expression vector pET28a::PfHsp90, pET28a::PfHsp70-1, and pProEx-HTa::ScHsp82 (a gift from Prof. Walid A. Houry, University of Toronto, CA) obtained from a previous study and purified until homogeneity, as previously described.<sup>82,83</sup> Recombinant ScSsa1 (NP\_009396.2) was expressed by the expression vector pET28aTEV::ScSsa1 (a gift from Prof. Carlos H. Inácio Ramos, University of Campinas, SP, Brazil) in the *E. coli* Bl21 (DE3) strain grown in LB medium containing 35  $\mu$ g/mL of kanamycin (up to OD<sub>600</sub> = 0.6–0.8) at 37 °C and 200 rpm. Induction was performed using 0.4 mM IPTG, with incubation at 20 °C and 200 rpm for 18 h. After induction, the cells were centrifuged, disrupted in the presence of 1 mM PMSF and the recombinant ScSsa1 protein was purified as described for PfHsp70-1.<sup>82</sup> The purity of all steps was assessed by 12% SDS-PAGE, and the His-tag on the recombinant proteins was kept. The amino acid sequences of the PfHsp70-1 and ScSsa1 proteins were aligned and the identity between them was obtained using the Clustal Omega program ([www.ebi.ac.uk/Tools/msa/clustalo/](http://www.ebi.ac.uk/Tools/msa/clustalo/)).

**4.2.12. Circular Dichroism (CD) for Analysis of PfHsp90–Violacein and PfHsp70-1–Violacein Interactions.** CD spectropolarimetry experiments were performed using a Jasco J-815 spectropolarimeter (Jasco, Inc.), under temperature control by a Peltier system. The far-UV CD was performed in a 1 mm quartz cuvette with a 0.2 mm path

length using a buffer composed of 40 mM HEPES-KCl (pH 7.5) and 100 mM KCl for PfHsp90 and ScHsp82 proteins and of 25 mM Tris-HCl (pH 7.5), 50 mM NaCl, 5 mM sodium phosphate, and 5 mM KCl for PfHsp70-1 and ScSsa1. Assays were performed using 2.5  $\mu$ M PfHsp90, PfHsp70-1, ScHsp82, and ScSsa1 proteins with 30 min preincubation of equimolar amounts of violacein and DMSO (controls). The values generated by the CD curves were converted to an ellipticity molar ratio ( $[\theta]$ ) as follows:

$$[\theta] = \frac{100\theta_{MM}}{Cl_n}$$

where  $[\theta]$  is the mean residual molar ellipticity (in deg cm<sup>2</sup>/dmol), MM is the molecular mass of the protein in kDa, C is the protein concentration (mg/mL), *l* is the optical path in cm, and *n* is the number of amino acid residues of the protein.

**4.2.13. Differential Scanning Calorimetry (DSC) for Chaperone–Violacein Interaction Analysis.** DSC was performed on a Nano DSC (TA Instruments), using the same buffer as described in section 4.2.12. PfHsp90 and PfHsp70-1 were exhaustively dialyzed and prepared to a concentration of 1.0–1.4 mg/mL. The thermal range used for DSC was 20–90 °C, with a temperature rise of 1 °C/min. The thermograms of the protein, preincubated or not with a molar concentration five times higher than that of violacein, were collected by DSC-Run software (TA Instruments) and data processing was performed using Launch NanoAnalyze software.

**4.2.14. ATPase Activity Assays.** The ATPase activity of both PfHsp90, PfHsp70-1, ScHsp82, and ScSsa1 proteins was tested under different concentrations of violacein. The tests with PfHsp90 and ScHsp82 were performed on a 96-well microplate with 40 mM HEPES buffer (pH 7.5) supplemented with 100 mM KCl. Assays with PfHsp70-1 and ScSsa1 proteins were performed in 50 mM Tris-HCl buffer (pH 7.5), 25 mM NaCl, and 5 mM KCl. The PfHsp90 (2.0  $\mu$ M) and PfHsp70-1 (2.5  $\mu$ M), ScHsp82 (2  $\mu$ M) and ScSsa1 (2.5  $\mu$ M) proteins were incubated for 30 min at 25 °C in the presence of 2 mM MgCl<sub>2</sub> under different concentrations of violacein (0–20  $\mu$ M). Then, 1 mM ATP was added, and the mixture was incubated in a water bath for 30 min at 37 °C. After the reaction, the solutions were incubated with a PiColorLock Gold kit Phosphate Detection System (Innova Biosciences) for 30 min at room temperature. In the ATPase activity assays performed with the proteins PfHsp90 and yHsp82, geldanamycin (GA) (0–20  $\mu$ M) was used as a positive control. Half of the maximum inhibitory concentration (IC<sub>50</sub>) was obtained by adjusting the dose response available in the Origin program (Microcal).

To analyze the type of inhibition resulting from violacein action on PfHsp70-1 and ScSsa1 proteins, kinetic assays of PfHsp70-1 (2.5  $\mu$ M) and ScSsa1 (2.5  $\mu$ M) were performed in the presence of 2 mM MgCl<sub>2</sub>, increasing ATP concentrations (0–1.0 mM) and two different violacein concentrations (1 and 5  $\mu$ M). The reactions were incubated for 30 min at 37 °C and subsequently treated with PiColorLock for 30 min at 25 °C. A standard curve was generated using increasing known values of free phosphate to provide an indirect data that correlates color and Pi concentration. After incubation, experimental readings were made in a Varioskan TM LUX multimode microplate reader (Thermo Fisher Scientific), with absorbance measurements in a range of 590–650 nm wavelength.

**4.2.15. Intrinsic Chaperone Activity Assays.** The intrinsic chaperone activities of PfHsp90, PfHsp70-1, ScHsp82, and ScSsa1 proteins were tested as previously described<sup>84</sup> to determine the ability to prevent thermal induced aggregation of the model client protein malate dehydrogenase (MDH) (porcine heart; Sigma; M2634). The ability of the two chaperones to avoid protein aggregation was assessed in the presence or absence of violacein and for the PfHsp90 and yHsp82 proteins using additionally assays with GA as positive control. In this test, 1  $\mu$ M MDH was subjected to a thermal stress of 42 °C for 3 h, in the absence or presence of PfHsp90, PfHsp70-1, ScHsp82, and ScSsa1 chaperones, pretreated or not with an equimolar dose of violacein for 30 min, and in the case of the PfHsp90 and yHsp82 using an equimolar dose of GA for 30 min. The experimental procedure was performed in 96-well plates and protein aggregation was measured by the readings of the light scattering signal at 320 nm in a Varioskan TM LUX multimode microplate reader (Thermo Fisher Scientific). All experiments were performed in the same buffer as that described in section 4.2.12. Experiments performed solely in the presence of MDH were used as controls, to determine the rate of aggregation of this protein in the absence of chaperones. The effect of violacein on the model protein thermal aggregation was also evaluated as a control.

**4.3. Statistical Analysis.** Statistical analysis was performed using Graphpad Prism software version 5.01. Sample sizes are described in figure legends. To calculate the EC<sub>50</sub> in parasites, a nonlinear regression curve was made with the data of the parasite survival in relation to control (percentage) and compound/drug concentration data expressed in logarithmic scale. For the membrane feeding assay, infection rates between groups were compared by one-way ANOVA and Kruskal–Wallis post-test. Data were considered statistically significant when  $p < 0.05$ . To all cases ( $n$ ) represents the number of independent biological replicates.

## ■ ASSOCIATED CONTENT

### Supporting Information

The Supporting Information is available free of charge at <https://pubs.acs.org/doi/10.1021/acsinfecdis.0c00454>.

*Plasmodium* TRiC- $\Theta$  knockdown assay (Figure S1). Violacein activity against *Plasmodium* in different stages (Table S1). Analysis of the primary structure of the PfHsp70-1 and ScSsa1 proteins (Figure S2). ATPase activity of PfHsp70-1 and ScSsa1 proteins in the presence of violacein (Figure S3). PfHsp90 and PfHsp70-1 thermal stability assays under violacein treatment (Table S2). MDH aggregation in the presence of Hsp70 chaperones and violacein (Table S3). Western blotting against p-eIF2 $\alpha$  (Figure S4) (PDF)

Table of resources (PDF)

## ■ AUTHOR INFORMATION

### Corresponding Author

**Fabio Trindade Maranhão Costa** – Laboratory of Tropical Diseases—Prof. Dr. Luiz Jacinto da Silva, Department of Genetics, Evolution, Microbiology and Immunology, University of Campinas—UNICAMP, Campinas, SP 13083-970, Brazil; [orcid.org/0000-0001-9969-7300](https://orcid.org/0000-0001-9969-7300); Email: [fabiomtmc72@gmail.com](mailto:fabiomtmc72@gmail.com)

## Authors

**Tatyana Almeida Tavella** – Laboratory of Tropical Diseases—Prof. Dr. Luiz Jacinto da Silva, Department of Genetics, Evolution, Microbiology and Immunology, University of Campinas—UNICAMP, Campinas, SP 13083-970, Brazil

**Noeli Soares Melo da Silva** – Biochemistry and Biophysics of Proteins Group—São Carlos Institute of Chemistry—IQSC, University of São Paulo, São Carlos, SP 13566-590, Brazil

**Natalie Spillman** – Department of Biochemistry, Bio 21 Institute, University of Melbourne, Melbourne, VIC 3052, Australia

**Ana Carolina Andrade Vitor Kayano** – Laboratory of Tropical Diseases—Prof. Dr. Luiz Jacinto da Silva, Department of Genetics, Evolution, Microbiology and Immunology, University of Campinas—UNICAMP, Campinas, SP 13083-970, Brazil

**Gustavo Capatti Cassiano** – Global Health and Tropical Medicine (GHTM), Instituto de Higiene e Medicina Tropical, Universidade Nova de Lisboa, 1099-085 Lisboa, Portugal; Laboratory of Tropical Diseases—Prof. Dr. Luiz Jacinto da Silva, Department of Genetics, Evolution, Microbiology and Immunology, University of Campinas—UNICAMP, Campinas, SP 13083-970, Brazil

**Adrielle Ayumi Vasconcelos** – Laboratory of Genomics and BioEnergy, Department of Genetics, Evolution, Microbiology and Immunology, Institute of Biology, University of Campinas—UNICAMP, Campinas, SP 13083-970, Brazil

**Antônio Pedro Camargo** – Laboratory of Genomics and BioEnergy, Department of Genetics, Evolution, Microbiology and Immunology, Institute of Biology, University of Campinas—UNICAMP, Campinas, SP 13083-970, Brazil

**Djane Clarys Baia da Silva** – Leônidas & Maria Deane Institute, Fundação Oswaldo Cruz—FIOCRUZ, Manaus, AM 69057070, Brazil; Fundação de Medicina Tropical—Dr. Heitor Vieira Dourado, Manaus, AM 69040-000, Brazil

**Diana Fontinha** – Instituto de Medicina Molecular João Lobo Antunes, Faculdade de Medicina, Universidade de Lisboa, 1649-004 Lisboa, Portugal

**Luis Carlos Salazar Alvarez** – Laboratory of Tropical Diseases—Prof. Dr. Luiz Jacinto da Silva, Department of Genetics, Evolution, Microbiology and Immunology, University of Campinas—UNICAMP, Campinas, SP 13083-970, Brazil

**Letícia Tiburcio Ferreira** – Laboratory of Tropical Diseases—Prof. Dr. Luiz Jacinto da Silva, Department of Genetics, Evolution, Microbiology and Immunology, University of Campinas—UNICAMP, Campinas, SP 13083-970, Brazil

**Kaira Cristina Peralis Tomaz** – Laboratory of Tropical Diseases—Prof. Dr. Luiz Jacinto da Silva, Department of Genetics, Evolution, Microbiology and Immunology, University of Campinas—UNICAMP, Campinas, SP 13083-970, Brazil

**Bruno Junior Neves** – Laboratory of Molecular Modeling and Drug Design, LabMol, Faculdade de Farmácia, Universidade Federal de Goiás, Goiânia, GO 74605-170, Brazil; LabChem—Laboratory of Cheminformatics, Centro Universitário de Anápolis—UniEVANGÉLICA, Anápolis, GO 75083-515, Brazil; [orcid.org/0000-0002-1309-8743](https://orcid.org/0000-0002-1309-8743)

**Ludimila Dias Almeida** – Synthetic Biology Laboratory, Department of Structural and Functional Biology, Institute of Biology, UNICAMP, Campinas, SP, Brazil

**Daniel Youssef Bargieri** – Department of Parasitology, Institute of Biomedical Sciences, University of São Paulo, Cidade Universitária “Armando Salles Oliveira”, São Paulo 05508-000, Brazil

**Marcus Vinicius Guimarães de Lacerda** – Fundação de Medicina Tropical–Dr. Heitor Vieira Dourado, Manaus, AM 69040-000, Brazil

**Pedro Vitor Lemos Cravo** – Global Health and Tropical Medicine (GHTM), Instituto de Higiene e Medicina Tropical, Universidade Nova de Lisboa, 1099-085 Lisboa, Portugal; LabChem–Laboratory of Cheminformatics, Centro Universitário de Anápolis–UniEVANGÉLICA, Anápolis, GO 75083-515, Brazil

**Per Sunnerhagen** – Department of Chemistry and Molecular Biology, University of Gothenburg, 405 30 Gothenburg, Sweden; [orcid.org/0000-0002-0967-8729](https://orcid.org/0000-0002-0967-8729)

**Miguel Prudêncio** – Instituto de Medicina Molecular João Lobo Antunes, Faculdade de Medicina, Universidade de Lisboa, 1649-004 Lisboa, Portugal

**Carolina Horta Andrade** – Laboratory of Tropical Diseases–Prof. Dr. Luiz Jacinto da Silva, Department of Genetics, Evolution, Microbiology and Immunology, University of Campinas–UNICAMP, Campinas, SP 13083-970, Brazil; Laboratory of Molecular Modeling and Drug Design, LabMol, Faculdade de Farmácia, Universidade Federal de Goiás, Goiânia, GO 74605-170, Brazil

**Stefanie Costa Pinto Lopes** – Leônidas & Maria Deane Institute, Fundação Oswaldo Cruz–FIOCRUZ, Manaus, AM 69057070, Brazil; Fundação de Medicina Tropical–Dr. Heitor Vieira Dourado, Manaus, AM 69040-000, Brazil

**Marcelo Falsarella Carazzolle** – Laboratory of Genomics and BioEnergy, Department of Genetics, Evolution, Microbiology and Immunology, Institute of Biology, University of Campinas–UNICAMP, Campinas, SP 13083-970, Brazil

**Leann Tilley** – Department of Biochemistry, Bio 21 Institute, University of Melbourne, Melbourne, VIC 3052, Australia; [orcid.org/0000-0001-9910-0199](https://orcid.org/0000-0001-9910-0199)

**Elizabeth Bilsland** – Synthetic Biology Laboratory, Department of Structural and Functional Biology, Institute of Biology, UNICAMP, Campinas, SP, Brazil

**Júlio César Borges** – Biochemistry and Biophysics of Proteins Group–São Carlos Institute of Chemistry–IQSC, University of São Paulo, São Carlos, SP 13566-590, Brazil; [orcid.org/0000-0003-4856-748X](https://orcid.org/0000-0003-4856-748X)

Complete contact information is available at: <https://pubs.acs.org/10.1021/acscinfecdis.0c00454>

### Author Contributions

▼ E.B. and J.C.B. contributed equally to the supervision of this work. T.A.T. conceptualized, designed, and conducted the experiments and wrote the paper. N.S.M.S. and N.S. designed and conducted the experiments. A.C.K., G.C.C., D.C.B.S., D.F., L.C.S., L.T.F., K.C.P.T., B.J.N., and D.Y.B. conducted experiments. L.D.A., A.A.V., A.P.C., and M.F.C. designed and processed CGP data. M.V.G.L., P.V.L.C., P.S., M.P., L.T., E.B., and J.C.B. provided resources and laboratory infrastructure. L.T., E.B., J.C.B., and F.T.M.C. supervised this work. E.B. and F.T.M.C. conceptualized this project. All authors reviewed the manuscript.

### Funding

This work was funded by Fundação de Amparo à Pesquisa do Estado de São Paulo (FAPESP), Conselho Nacional de Desenvolvimento Científico e Tecnológico (CNPq), and Coordenação de Aperfeiçoamento de Pessoal de Nível Superior (CAPES). Fundação para a Ciência e Tecnologia, Portugal (FCT) grant PTDC-SAU-INF-29550-2017 supported M.P. and grant PTDC/SAU-PAR/28459/2017 supported P.V.L.C. F.T.M.C. and C.H.A. are research fellows in productivity of CNPq. F.T.M.C. is supported by the Fundação de Amparo à Pesquisa do Estado de São Paulo (FAPESP; grant 2017/18611-7). E.B. was supported by FAPESP (2015/03553-6 and 2018/07007-4). T.A.T. was supported by CAPES and FAPESP (2019/27626-3). E.B., F.T.M.C., and P.S. were supported by the Swedish Research Council (grant 2016-05627). L.T.F., G.C.C., and K.C.P.T. were supported by FAPESP fellowships (2019/02171-3, 2015/20774-6, and 2018/24878-9, respectively). L.C.S.A. and N.S.M.S. were supported by CNPq fellowships (162117/2018-3 and 141986/2017-4, respectively). L.D.A., A.A.V., and A.P.C. were supported by FAPESP fellowships (2017/01986-8, 2017/13015-7, and 2018/04240-0, respectively). S.C.P.L. was supported by CNPq fellowship (442849/2019-2) and by FIOCRUZ (Programa INOVA Novos Talentos). D.C.B.S. was supported by FAPEAM (Edital 002/2018). M.F.C. was supported by FAPESP/CEPID (2013/08293-7). D.Y.B. is supported by FAPESP (2013/13119-6) and Instituto Serrapilheira (G-1709-16618). The J.C.B. lab is also supported by FAPESP (2012/50161-8, 2017/07335-9, and 2017/26131-5). B.J.N. and C.H.A. were supported by the Brazilian CNPq/FAPEG (grant 300508/2017-4). L.T. and N.S. (NHMRC APP1072217) were supported by the Australian National Health and Medical Research Council (NHMRC). The funding agencies had no role in study design; in data collection, analysis, and interpretation of data; in the writing of the report; and in the decision to submit the paper for publication.

### Notes

The authors declare no competing financial interest. The BioProject accession number of the SRA database generated from this work is PRJNA689872. In order to guarantee reproducibility of our results, all the code we used to process the data is available in a public databank (<https://zenodo.org/record/4443837>). To access our CGP data set, Violacein vs Control: <https://data.mendeley.com/datasets/Sptks9t6b7/4>

### ACKNOWLEDGMENTS

The authors would like to thank Brazilian funding agencies, FAPESP, CAPES, CNPq, and FAPEG, for financial support and fellowships. The authors would like to thank Prof. Dr. Gerhard Wunderlich for brilliant insights that contributed to improving the quality of this work, BioPic3D for figure design, and Insight Editing London for language editing the manuscript prior to submission.

### REFERENCES

- (1) World Health Organization. *World Malaria Report 2019*; Geneva, 2019.
- (2) Cowman, A. F., Healer, J., Marapana, D., and Marsh, K. (2016) Review Malaria: Biology and Disease. *Cell* 167 (3), 610–624.

- (3) Derbyshire, E. R., Mota, M. M., and Clardy, J. (2011) The Next Opportunity in Anti-Malaria Drug Discovery: The Liver Stage. *PLoS Pathog.*, DOI: 10.1371/journal.ppat.1002178.
- (4) Delves, M. J., Angrisano, F., and Blagborough, A. M. (2018) Antimalarial Transmission-Blocking Interventions: Past, Present, and Future. *Trends Parasitol.* 34 (9), 735–746.
- (5) *Malaria: Strategy Overview*; Bill Melinda Gates Foundation, 2011; April, pp 1–6.
- (6) Brown, G. C. (1991) Total Cell Protein Concentration as an Evolutionary Constraint on the Metabolic Control Distribution in Cells. *J. Theor. Biol.* 153 (2), 195–203.
- (7) Zwanzig, R., Szabo, A., and Bagchi, B. (1992) Levinthal's Paradox. *Proc. Natl. Acad. Sci. U. S. A.* 89 (1), 20–22.
- (8) Hartl, F. U., Bracher, A., and Hayer-Hartl, M. (2011) Molecular Chaperones in Protein Folding and Proteostasis. *Nature* 475, 324–332.
- (9) Gulukota, K., and Wolynes, P. G. (1994) Statistical Mechanics of Kinetic Proofreading in Protein Folding in Vivo. *Proc. Natl. Acad. Sci. U. S. A.* 91 (20), 9292–9296.
- (10) Jortzik, E., and Becker, K. (2012) Thioredoxin and Glutathione Systems in Plasmodium Falciparum. *Int. J. Med. Microbiol.* 302 (4–5), 187–194.
- (11) Becker, K., Tilley, L., Vennerstrom, J. L., Roberts, D., Rogerson, S., and Ginsburg, H. (2004) Oxidative Stress in Malaria Parasite-Infected Erythrocytes: Host - Parasite Interactions. *Int. J. Parasitol.* 34 (2), 163–189.
- (12) Acharya, P., Kumar, R., and Tatu, U. (2007) Chaperoning a Cellular Upheaval in Malaria: Heat Shock Proteins in Plasmodium Falciparum. *Mol. Biochem. Parasitol.* 153 (2), 85–94.
- (13) Pavithra, S. R., Kumar, R., and Tatu, U. (2007) Systems Analysis of Chaperone Networks in the Malarial Parasite Plasmodium Falciparum. *PLoS Comput. Biol.* 3 (9), 1701–1715.
- (14) Dogovski, C., Xie, S. C., Burgio, G., Bridgford, J., Mok, S., McCaw, J. M., Chotivanich, K., Kenny, S., Gnädig, N., Straimer, J., Bozdech, Z., Fidock, D. A., Simpson, J. A., Dondorp, A. M., Foote, S., Klonis, N., and Tilley, L. (2015) Targeting the Cell Stress Response of Plasmodium Falciparum to Overcome Artemisinin Resistance. *PLoS Biol.* 13 (4), e1002132.
- (15) Gosline, S. J. C., Nascimento, M., McCall, L. I., Zilberstein, D., Thomas, D. Y., Matlashewski, G., and Hallett, M. (2011) Intracellular Eukaryotic Parasites Have a Distinct Unfolded Protein Response. *PLoS One*, DOI: 10.1371/journal.pone.0019118.
- (16) Posfai, D., Eubanks, A. L., Keim, A. I., Lu, K. Y., Wang, G. Z., Hughes, P. F., Kato, N., Haystead, T. A., and Derbyshire, E. R. (2018) Identification of Hsp90 Inhibitors with Anti-Plasmodium Activity. *Antimicrob. Agents Chemother.* 62 (4), No. e01799-17.
- (17) Wang, T., Mäser, P., and Picard, D. (2016) Inhibition of Plasmodium Falciparum Hsp90 Contributes to the Antimalarial Activities of Aminoalcohol-Carbazoles. *J. Med. Chem.* 59 (13), 6344–6352.
- (18) Neckers, L., and Tatu, U. (2008) Molecular Chaperones in Pathogen Virulence: Emerging New Targets for Therapy. *Cell Host Microbe* 4 (6), 519–527.
- (19) Shonhai, A. (2010) Plasmodial Heat Shock Proteins: Targets for Chemotherapy. *FEMS Immunol. Med. Microbiol.* 58 (1), 61–74.
- (20) Meshnick, S. R., and Dobson, M. J. (2001) The History of Antimalarial Drugs. *Antimalarial Chemotherapy* 0, 15–25.
- (21) Achan, J., Talisuna, A. O., Erhart, A., Yeka, A., Tibenderana, J. K., Baliraine, F. N., Rosenthal, P. J., and D'Alessandro, U. (2011) Quinine, an Old Anti-Malarial Drug in a Modern World: Role in the Treatment of Malaria. *Malar. J.* 10 (1), 144.
- (22) Tu, Y. (2011) The Discovery of Artemisinin (Qinghaosu) and Gifts from Chinese Medicine. *Nat. Med.* 17 (10), 1217–1220.
- (23) Ginsburg, H., and Deharo, E. (2011) A Call for Using Natural Compounds in the Development of New Antimalarial Treatments - an Introduction. *Malar. J.*, DOI: 10.1186/1475-2875-10-S1-S1.
- (24) Cauz, A. C. G., Carretero, G. P. B., Saraiva, G. K. V., Park, P., Mortara, L., Cuccovia, I. M., Brocchi, M., and Gueiros-Filho, F. J. (2019) Violacein Targets the Cytoplasmic Membrane of Bacteria. *ACS Infect. Dis.* 5 (4), 539–549.
- (25) Bilsland, E., Tavella, T. A., Krogh, R., Stokes, J. E., Roberts, A., Ajioka, J., Spring, D. R., Andricopulo, A. D., Costa, F. T. M., and Oliver, S. G. (2018) Antiplasmodial and Trypanocidal Activity of Violacein and Deoxyviolacein Produced from Synthetic Operons. *BMC Biotechnol.* 18 (1), 22.
- (26) Durán, M., Justo, G. Z., Durán, M., Brocchi, M., Cordi, L., Tasic, L., Castro, G. R., and Nakazato, G. (2016) Advances in Chromobacterium Violaceum and Properties of Violacein-Its Main Secondary Metabolite: A Review. *Biotechnol. Adv.* 34 (5), 1030–1045.
- (27) Lopes, S. C. P., Blanco, Y. C., Justo, G. Z., Nogueira, P. A., Rodrigues, F. L. S., Goelnitz, U., Wunderlich, G., Facchini, G., Brocchi, M., Duran, N., and Costa, F. T. M. (2009) Violacein Extracted from Chromobacterium Violaceum Inhibits Plasmodium Growth in Vitro and in Vivo. *Antimicrob. Agents Chemother.* 53 (5), 2149–2152.
- (28) Gitau, G. W., Mandal, P., Blatch, G. L., Przyborski, J., and Shonhai, A. (2012) Characterisation of the Plasmodium Falciparum Hsp70-Hsp90 Organising Protein (PfHop). *Cell Stress Chaperones* 17 (2), 191–202.
- (29) Daniyan, M. O., Przyborski, J. M., and Shonhai, A. (2019) Partners in Mischief: Functional Networks of Heat Shock Proteins of Plasmodium Falciparum and Their Influence on Parasite Virulence. *Biomolecules* 9 (7), 295.
- (30) Veiga, M. I., Dhingra, S. K., Henrich, P. P., Straimer, J., Gnädig, N., Uhlemann, A. C., Martin, R. E., Lehane, A. M., and Fidock, D. A. (2016) Globally Prevalent PfMDR1 Mutations Modulate Plasmodium Falciparum Susceptibility to Artemisinin-Based Combination Therapies. *Nat. Commun.* 7, 11553.
- (31) Ecker, A., Lehane, A. M., Clain, J., and Fidock, D. A. (2012) PfCRT and Its Role in Antimalarial Drug Resistance. *Trends Parasitol.* 28 (11), 504–514.
- (32) Triglia, T., Foote, S. J., Kemp, D. J., and Cowman, A. F. (1991) Amplification of the Multidrug Resistance Gene Pfmdr1 in Plasmodium Falciparum Has Arisen as Multiple Independent Events. *Mol. Cell. Biol.* 11 (10), 5244–5250.
- (33) Le Manach, C., Scheurer, C., Sax, S., Schleiferböck, S., Cabrera, D. G., Younis, Y., Paquet, T., Street, L., Smith, P., Ding, X. C., Waterson, D., Witty, M. J., Leroy, D., Chibale, K., and Wittlin, S. (2013) Fast in Vitro Methods to Determine the Speed of Action and the Stage-Specificity of Anti-Malarials in Plasmodium Falciparum. *Malar. J.* 12 (1), 424.
- (34) Butterworth, A. S., Skinner-Adams, T. S., Gardiner, D. O. N. L., and Trenholme, K. R. (2013) Plasmodium Falciparum Gametocytes: With a View to a Kill. *Parasitology* 140 (14), 1718–1734.
- (35) Capela, R., Magalhães, J., Miranda, D., Machado, M., Sanches-Vaz, M., Albuquerque, I. S., Sharma, M., Gut, J., Rosenthal, P. J., Frade, R., Perry, M. J., Moreira, R., M. Prudêncio, F. L., et al. (2018) Endoperoxide-8-Aminoquinoline Hybrids as Dual-Stage Antimalarial Agents with Enhanced Metabolic Stability. *Eur. J. Med. Chem.* 149 (149), 69–78.
- (36) Park, E. C., Finley, D., and Szostak, J. W. (1992) A Strategy for the Generation of Conditional Mutations by Protein Destabilization. *Proc. Natl. Acad. Sci. U. S. A.* 89 (4), 1249–1252.
- (37) Parsons, A. B., Brost, R. L., Ding, H., Li, Z., Zhang, C., Sheikh, B., Brown, G. W., Kane, P. M., Hughes, T. R., and Boone, C. (2004) Integration of Chemical-Genetic and Genetic Interaction Data Links Bioactive Compounds to Cellular Target Pathways. *Nat. Biotechnol.* 22 (1), 62–69.
- (38) Giaever, G., Shoemaker, D. D., Jones, T. W., Liang, H., Winzler, E. A., Astromoff, A., and Davis, R. W. (1999) Genomic Profiling of Drug Sensitivities via Induced Haploinsufficiency. *Nat. Genet.* 21 (3), 278–283.
- (39) Smith, A. M., Heisler, L. E., St. Onge, R. P., Farias-Hesson, E., Wallace, I. M., Bodeau, J., Harris, A. N., Perry, K. M., Giaever, G., Pourmand, N., and Nislow, C. (2010) Highly-Multiplexed Barcode

Sequencing: An Efficient Method for Parallel Analysis of Pooled Samples. *Nucleic Acids Res.* 38 (13), e142.

(40) Hoepfner, D., McNamara, C. W., Lim, C. S., Studer, C., Riedl, R., Aust, T., McCormack, S. L., Plouffe, D. M., Meister, S., Schuierer, S., Plikat, U., Hartmann, N., Staedtler, F., Cotesta, S., Schmitt, E. K., Petersen, F., Supek, F., Glynne, R. J., Tallarico, J. A., Porter, J. A., Fishman, M. C., Bodenreider, C., Diagana, T. T., Movva, N. R., and Winzeler, E. A. (2012) Selective and Specific Inhibition of the Plasmodium Falciparum Lysyl-TRNA Synthetase by the Fungal Secondary Metabolite Cladosporin. *Cell Host Microbe* 11 (6), 654–663.

(41) Rodger, A., Marrington, R., Roper, D., and Windsor, S. (2005) Circular Dichroism Spectroscopy for the Study of Protein-Ligand Interactions. *Methods Mol. Biol.* 305, 343–363.

(42) Zsila, F. (2013) Circular Dichroism Spectroscopic Detection of Ligand Binding Induced Subdomain IB Specific Structural Adjustment of Human Serum Albumin. *J. Phys. Chem. B* 117 (37), 10798–10806.

(43) Minari, K., de Azevedo, E. C., Kiraly, V. T. R., Batista, F. A. H., de Moraes, F. R., de Melo, F. A., Nascimento, A. S., Gava, L. M., Ramos, C. H. L., and Borges, J. C. (2019) Thermodynamic Analysis of Interactions of the Hsp90 with Adenosine Nucleotides: A Comparative Perspective. *Int. J. Biol. Macromol.* 130, 125–138.

(44) Silva, K. P., Seraphim, T. V., and Borges, J. C. (2013) Structural and Functional Studies of Leishmania Braziliensis Hsp90. *Biochim. Biophys. Acta, Proteins Proteomics* 1834 (1), 351–361.

(45) Montgomery, D. L., Morimoto, R. I., and Gierasch, L. M. (1999) Mutations in the Substrate Binding Domain of the Escherichia Coli 70 kDa Molecular Chaperone, DnaK, Which Alter Substrate Affinity or Interdomain Coupling. *J. Mol. Biol.* 286 (3), 915–932.

(46) Batinovic, S., McHugh, E., Chisholm, S. A., Matthews, K., Liu, B., Dumont, L., Charnaud, S. C., Schneider, M. P., Gilson, P. R., De Koning-Ward, T. F., Dixon, M. W. A., and Tilley, L. (2017) An Exported Protein-Interacting Complex Involved in the Trafficking of Virulence Determinants in Plasmodium-Infected Erythrocytes. *Nat. Commun.* 8 (1), 16044.

(47) Roe, S. M., Prodrromou, C., O'Brien, R., Ladbury, J. E., Piper, P. W., and Pearl, L. H. (1999) Structural Basis for Inhibition of the Hsp90 Molecular Chaperone by the Antitumor Antibiotics Radicol and Geldanamycin. *J. Med. Chem.* 42 (2), 260–266.

(48) Stebbins, C. E., Russo, A. A., Schneider, C., Rosen, N., Hartl, F. U., and Pavletich, N. P. (1997) Crystal Structure of an Hsp90 - Geldanamycin Complex: Targeting of a Protein Chaperone by an Antitumor Agent. *Cell* 89 (2), 239–250.

(49) Whitesell, L., Miwnaugh, E. G., De Costa, B., Myers, C. E., and Neckers, L. M. (1994) Inhibition of Heat Shock Protein HSP90-Pp60v-Src Heteroprotein Complex Formation by Benzoquinone Ansamycins: Essential Role for Stress Proteins in Oncogenic Transformation. *Proc. Natl. Acad. Sci. U. S. A.* 91 (18), 8324–8328.

(50) Li, J., Soroka, J., and Buchner, J. (2012) The Hsp90 Chaperone Machinery: Conformational Dynamics and Regulation by Co-Chaperones. *Biochim. Biophys. Acta, Mol. Cell Res.* 1823, 624–635.

(51) Silva, K. P., and Borges, J. C. (2011) The Molecular Chaperone Hsp70 Family Members Function by a Bidirectional Heterotropic Allosteric Mechanism. *Protein Pept. Lett.* 18 (2), 132–142.

(52) Young, J. C. (2010) Mechanisms of the Hsp70 Chaperone System. *Biochem. Cell Biol.* 88 (2), 291–300.

(53) Clerico, E. M., Tilitsky, J. M., Meng, W., and Gierasch, L. M. (2015) How Hsp70 Molecular Machines Interact with Their Substrates to Mediate Diverse Physiological Functions. *J. Mol. Biol.* 427 (7), 1575–1588.

(54) Kityk, R., Kopp, J., Sinning, I., and Mayer, M. P. (2012) Structure and Dynamics of the ATP-Bound Open Conformation of Hsp70 Chaperones. *Mol. Cell* 48 (6), 863–874.

(55) Liberek, K., Lewandowska, A., and Zietkiewicz, S. (2008) Chaperones in Control of Protein Disaggregation. *EMBO J.* 27 (2), 328–335.

(56) Silva, K. P., Seraphim, T. V., and Borges, J. C. (2013) Structural and Functional Studies of Leishmania Braziliensis Hsp90. *Biochim. Biophys. Acta, Proteins Proteomics* 1834 (1), 351–361.

(57) Kravats, A. N., Hoskins, J. R., Reidy, M., Johnson, J. L., Doyle, S. M., Genest, O., Masison, D. C., and Wickner, S. (2018) Functional and Physical Interaction between Yeast Hsp90 and Hsp70. *Proc. Natl. Acad. Sci. U. S. A.* 115 (10), E2210–E2219.

(58) Leu, J. I., Pimkina, J., Pandey, P., Murphy, M. E., and George, D. L. (2011) HSP70 Inhibition by the Small-Molecule 2-Phenylethanesulfonamide Impairs Protein Clearance Pathways in Tumor Cells. *Mol. Cancer Res.* 9 (7), 936–948.

(59) Leu, J. I., Pimkina, J., Frank, A., Murphy, M. E., and George, D. L. (2009) A Small Molecule Inhibitor of Inducible Heat Shock Protein 70 (HSP70). *Mol. Cell* 36 (1), 15–27.

(60) Galluzzi, L., Diotallevi, A., and Magnani, M. (2017) Endoplasmic Reticulum Stress and Unfolded Protein Response in Infection by Intracellular Parasites. *Futur. Sci. OA* 3 (3), FSO198.

(61) Bridgford, J. L., Xie, S. C., Cobbold, S. A., Pasaje, C. F. A., Herrmann, S., Yang, T., Gillett, D. L., Dick, L. R., Ralph, S. A., Spillman, N. J., Tilley, L., and Dogovski, C. (2018) Artemisinin Kills Malaria Parasites by Damaging Proteins and Inhibiting the Proteasome. *Nat. Commun.* 9, 3801.

(62) Xie, S. C., Gillett, D. L., Spillman, N. J., Tsu, C., Luth, M. R., Ottilie, S., Duffy, S., Gould, A. E., Hales, P., Seager, B. A., Charron, C. L., Bruzzese, F., Yang, X., Zhao, X., Huang, S.-C., Hutton, C. A., Burrows, J. N., Winzeler, E. A., Avery, V. M., Dick, L. R., and Tilley, L. (2018) Target Validation and Identification of Novel Boronate Inhibitors of the Plasmodium Falciparum Proteasome. *J. Med. Chem.* 61 (22), 10053–10066.

(63) Buchberger, A., Bukau, B., and Sommer, T. (2010) Protein Quality Control in the Cytosol and the Endoplasmic Reticulum: Brothers in Arms. *Mol. Cell* 40 (2), 238–252.

(64) Antonova-Koch, Y., Meister, S., Abraham, M., Luth, M. R., Ottilie, S., Lukens, A. K., Sakata-Kato, T., Vanaerschot, M., Owen, E., Jado Rodriguez, J. C., Maher, S. P., Calla, J., Plouffe, D., Zhong, Y., Chen, K., Chaumeau, V., Conway, A. J., McNamara, C. W., Ibanez, M., Gagaring, K., Serrano, F. N., Eribe, K., Taggard, C. M. L., Cheung, A. L., Lincoln, C., Ambachew, B., Rouillier, M., Siegel, D., Nosten, F., Kyle, D. E., Gamo, F. J., Zhou, Y., Llinás, M., Fidock, D. A., Wirth, D. F., Burrows, J., Campo, B., and Winzeler, E. A. (2018) Open-Source Discovery of Chemical Leads for next-Generation Chemoprotective Antimalarials. *Science* 362 (6419), eaat9446.

(65) Bermúdez, M., Andrés, D., Pérez, M., Pinzón, G. A., Curtidor, H., and Patarroyo, M. A. (2018) Plasmodium Vivax in Vitro Continuous Culture: The Spoke in the Wheel. *Malar. J.*, 1–12.

(66) Bousema, T., and Drakeley, C. (2011) Epidemiology and Infectivity of Plasmodium Falciparum and Plasmodium Vivax Gametocytes in Relation to Malaria Control and Elimination. *Clin. Microbiol. Rev.* 24 (2), 377–410.

(67) Moran Luengo, T., Mayer, M. P., and Rudiger, S. G.D. (2019) The Hsp70 - Hsp90 Chaperone Cascade in Protein Folding. *Trends Cell Biol.* 29 (2), 164–177.

(68) Wilkinson, M. D., Lai, H.-E., Freemont, P. S., and Baum, J. (2020) A Biosynthetic Platform for Antimalarial Drug Discovery. *Antimicrob. Agents Chemother.*, DOI: 10.1128/AAC.02129-19.

(69) Neckers, L., and Workman, P. (2012) Hsp90 Molecular Chaperone Inhibitors: Are We There Yet? *Clin. Cancer Res.* 18 (1), 64–76.

(70) Gestwicki, J. E., and Shao, H. (2019) Inhibitors and Chemical Probes for Molecular Chaperone Networks. *J. Biol. Chem.* 294 (6), 2151–2161.

(71) Trager, W., and Jensen, J. B. (1976) Human Malaria Parasites in Continuous Culture. *Science (Washington, DC, U. S.)* 193 (4254), 673–675.

(72) Ploemen, I. H., Prudêncio, M., Douradinha, B. G., Ramesar, J., Fonager, J., van Gemert, G. J., Luty, A. J., Hermsen, C. C., Sauerwein,

R. W., Baptista, F. G., Mota, M. M., Waters, A. P., Que, I., Lowik, C. W., Khan, S. M., C.J. Janse, B. M. F.-F., et al. (2009) Visualization and Quantitative Analysis of the Rodent Malaria Liver Stage by Real Time Imaging. *PLoS One* 4 (11), No. e7881.

(73) Pimenta, P. F. P., Orfano, A. S., Bahia, A. C., Duarte, A. P. M., Rios-Velázquez, C. M., Melo, F. F., Pessoa, F. A. C., Oliveira, G. A., Campos, K. M. M., Villegas, L. M., Rodrigues, N. B., Nacif-pimenta, R., Simões, R. C., Monteiro, W. M., Amino, R., Traub-cseko, Y. M., Lima, J. B. P., Barbosa, M. G. V., Lacerda, M. V. G., Tadei, W. P., and Secundino, N. F. C. (2015) An Overview of Malaria Transmission from the Perspective of Amazon Anopheles Vectors. *Mem. Inst. Oswaldo Cruz* 110 (1), 23–47.

(74) Hartwig, C. L. et al. (2013) BYBR Green I-Based Parasite Growth Inhibition Assay for Measurement of Antimalarial Drug Susceptibility in *Plasmodium Falciparum*. *Methods in Malaria Research*, pp 122–129.

(75) Dearnley, M. K., Yeoman, J. A., Hanssen, E., Kenny, S., Turnbull, L., Whitchurch, C. B., Tilley, L., and Dixon, M. W. A. (2012) Origin, Composition, Organization and Function of the Inner Membrane Complex of *Plasmodium Falciparum* Gametocytes. *J. Cell Sci.* 125 (8), 2053–2063.

(76) Dixon, M. W. A., Dearnley, M. K., Hanssen, E., Gilberger, T., and Tilley, L. (2012) Shape-Shifting Gametocytes: How and Why Does *P. Falciparum* Go Banana-Shaped? *Trends Parasitol.* 28 (11), 471–478.

(77) Schneekloth, J. S., Fonseca, F. N., Koldobskiy, M., Mandal, A., Deshaies, R., Sakamoto, K., and Crews, C. M. (2004) Chemical Genetic Control of Protein Levels: Selective in Vivo Targeted Degradation. *J. Am. Chem. Soc.* 126 (12), 3748–3754.

(78) Magariños, M. P., Carmona, S. J., Crowther, G. J., Ralph, S. A., Roos, D. S., Shanmugam, D., Van Voorhis, W. C., and Agüero, F. (2012) TDR Targets: A Chemogenomics Resource for Neglected Diseases. *Nucleic Acids Res.* 40 (D1), D1118–1127.

(79) Hoepfner, D., Helliwell, S. B., Sadlish, H., Schuierer, S., Filipuzzi, I., Brachat, S., Bhullar, B., Plikat, U., Abraham, Y., Altorfer, M., Aust, T., Baeriswyl, L., Cerino, R., Chang, L., Estoppey, D., Eichenberger, J., Frederiksen, M., Hartmann, N., Hohendahl, A., Knapp, B., Krastel, P., Melin, N., Nigsch, F., Oakeley, E. J., Petitjean, V., Petersen, F., Riedl, R., Schmitt, E. K., Staedtler, F., Studer, C., Tallarico, J. A., Wetzel, S., Fishman, M. C., Porter, J. A., and Movva, N. R. (2014) High-Resolution Chemical Dissection of a Model Eukaryote Reveals Targets, Pathways and Gene Functions. *Microbiol. Res.* 169 (2–3), 107–120.

(80) Love, M. I., Huber, W., and Anders, S. (2014) Moderated Estimation of Fold Change and Dispersion for RNA-Seq Data with DESeq2. *Genome Biol.* 15 (12), 1–21.

(81) Smith, A. M., Durbic, T., Oh, J., Urbanus, M., Proctor, M., Heisler, L. E., Giaever, G., and Nislow, C. (2011) Competitive Genomic Screens of Barcoded Yeast Libraries. *J. Vis. Exp.* 54, 2864.

(82) Silva, N. S.M., Bertolino-Reis, D. E., Dores-Silva, P. R., Anneta, F. B., Seraphim, T. V., Barbosa, L. R.S., and Borges, J. C. (2020) Structural Studies of the Hsp70/Hsp90 Organizing Protein of *Plasmodium Falciparum* and Its Modulation of Hsp70 and Hsp90 ATPase Activities. *Biochim. Biophys. Acta, Proteins Proteomics* 1868, 140282.

(83) Silva, N. S.M., Seraphim, T. V., Minari, K., Barbosa, L. R.S., and Borges, J. C. (2018) Comparative Studies of the Low-Resolution Structure of Two P23 Co-Chaperones for Hsp90 Identified in *Plasmodium Falciparum* Genome. *Int. J. Biol. Macromol.* 108, 193–204.

(84) Seraphim, T. V., Gava, L. M., Mokry, D. Z., Cagliari, T. C., Barbosa, L. R. S., Ramos, C. H. I., and Borges, J. C. (2015) The C-Terminal Region of the Human P23 Chaperone Modulates Its Structure and Function. *Arch. Biochem. Biophys.* 565, 57–67.